

AD-751 566

ASPECTS OF MECHANICAL BEHAVIOR OF ROCK
UNDER STATIC AND CYCLIC LOADING. PART A.
MECHANICAL BEHAVIOR OF ROCK UNDER STATIC
LOADING

Jesus Basas, et al

Wisconsin University

Prepared for:

Bureau of Mines
Advanced Research Projects Agency

September 1972

DISTRIBUTED BY:

NTIS

National Technical Information Service
U. S. DEPARTMENT OF COMMERCE
5285 Port Royal Road, Springfield Va. 22151

**BEST
AVAILABLE COPY**

ENGINEERING EXPERIMENT STATION

AD 751566

ASPECTS OF MECHANICAL BEHAVIOR OF ROCK UNDER STATIC AND CYCLIC LOADING

Part A Mechanical Behavior of Rock Under Static Loading

Semi-Annual Technical Progress Report
September 1972

Sponsored by Advanced Research Projects Agency
and monitored by U. S. Bureau of Mines
under Contract No. HG220041

ARPA Order No. 1579, Amendment 3
Program Code 62701D



DDC
NOV 16 1972

Reproduced by
NATIONAL TECHNICAL
INFORMATION SERVICE
U.S. Department of Commerce
Springfield VA 22151

DISTRIBUTION STATEMENT A
Approved for public release;
Distribution Unlimited

**ASPECTS OF MECHANICAL BEHAVIOR OF ROCK UNDER
STATIC AND CYCLIC LOADING**

PART A: MECHANICAL BEHAVIOR OF ROCK UNDER STATIC LOADING

**Semi-Annual Technical Progress Report
September 1972**

by

**R. W. Heins (Co-Principal Investigator
with B. C. Haimson)**

**Department of Metallurgical & Mineral Engineering
and the
Engineering Experiment Station
College of Engineering
The University of Wisconsin
Madison, Wisconsin 53706**

**ARPA Order No. 1579, Amendment 3
Program Code No. 62701D, Contract No. H0220041
Contract Period: March 1972 through April 1973
Total Amount of Contract: \$50,000
Sponsored by ARPA and Monitored by U. S. Bureau of Mines**

Disclaimer:

**The views and conclusions contained in this document are those of
the author and should not be interpreted as necessarily representing
the official policies, either expressed or implied, of the Advanced
Research Projects Agency or the U. S. Government.**

IC

Mar 7, 66

DOCUMENT CONTROL DATA - R & D	
<small>(The title of this report, the name of the organization, and the name of the author should be included when the overall report is classified)</small> Engineering Experiment Station University of Wisconsin Madison, Wisconsin - 53706	
SECURITY CLASSIFICATION Unclassified <small>7B. GROUP</small>	
Aspects of Mechanical Behavior of Rock under Static and Cyclic Loading Part A - Mechanical Behavior of Rock under Static Loading	
<small>4. DESCRIPTIVE NOTES (Type of report and inclusive dates)</small> Semi-Annual Technical Report <small>5. AUTHOR(S) (First name, middle initial, last name)</small> Jesus Basas, A. Hayatdavoudi, Robert W. Heins	
<small>6. REPORT DATE</small> September 1972	<small>7A. TOTAL NO. OF PAGES</small> 26 87
<small>7B. CONTRACT OR GRANT NO.</small> H0220041 <small>A. PROJECT NO.</small>	<small>8. ORIGINATOR'S REPORT NUMBER(S)</small> 144-C745 <small>9. OTHER REPORT NO(S) (Any other numbers that may be assigned this report)</small>
<small>10. INSTITUTION STATEMENT</small> Distribution of this document is unlimited.	
<small>11. SUPPLEMENTARY NOTES</small>	<small>12. SPONSORING MILITARY ACTIVITY</small> Advanced Research Projects Agency Washington, DC 20301
<small>13. ABSTRACT</small> <p>Brazilian tests were carried out to determine size-tensile strength dependence in dacite, Valders limestone, and St. Cloud gray granodiorite. It was concluded that there is a size effect on tensile strength; in Brazilian test, this effect is governed mainly by the position and orientation of the internal flaws relative to the loaded diametral plane.</p> <p>A two-dimensional computer program simulating the Brazilian test was written. The program employs four-sided, isoparametric elements and is based on the same failure criteria used in the first annual progress report. The present program, however, is more efficient and contains several features not found in the first program. Test runs have proven that the program can predict accurately the progression of failure in Brazilian test and, to a lesser extent, the correlation of load and displacement.</p> <p>A program employing both two-dimensional and three-dimensional elements is proposed. The program will be based on more realistic failure criteria and will take into account rock anisotropy.</p>	

DD FORM 1473
NOV 65

Details of illustrations in
 this document may be better
 studied on microfiche

IA

Security Classification

<p>finite element analysis Brazilian test indirect tensile strength model of rock failure force-displacement curve bounded distributions of strength and stiffness finite element progressive failure model</p>						

Ib

PREFACE

This report covers the first six months accomplishments in the research program entitled, "Mechanical Behavior of Rock Under Static Loading," R. W. Heins, Co-Principal Investigator. The program is Part A of the project entitled, "Aspects of Mechanical Behavior of Rock Under Static and Cyclic Loading" (Contract No. H020041). Part B of the project is published in a separate volume.

SUMMARY

ASPECTS OF MECHANICAL BEHAVIOR OF ROCK UNDER STATIC LOADING

PART A

Summary of Work to Date

Brazilian tests were carried out on three rocks (dacite, Valders limestone, and St. Cloud gray granodiorite) to determine size-tensile strength dependence. Plots of tensile strength versus specimen dimension (length or diameter) are shown in Chapter 1. It was concluded that there is a size effect on tensile strength; in Brazilian test, this effect is governed mainly by the position and orientation of the internal flaws relative to the loaded diametral plane rather than by the extent and number of the flaws.

A two-dimensional computer program simulating the Brazilian test has been completed. The program employs four-sided, isoparametric elements and is based on the same failure criteria described in the first annual progress report. The present program, however, is more efficient and contains several features not found in the first program. Test runs have proven that the program can predict accurately the progression of failure in Brazilian test and, to a lesser extent, the correlation of load and displacement.

Development of a program employing both two-dimensional and three-dimensional elements has started. The program will be based on more realistic failure criterion and will take into account rock anisotropy. Most of the writing of the program has been done and debugging of the program is in progress.

Future Work

Development of the combined two- or three-dimensional program will continue. Several examples will be run to check the correctness of the program.

TABLE OF CONTENTS

PREFACE	i
SUMMARY	ii
TABLE OF CONTENTS	iv
LIST OF FIGURES	v
LIST OF TABLES	vi
CHAPTER 1 - SIZE EFFECT ON BRAZILIAN TEST	1
1.1 Introduction	1
1.2 Experimental Procedure and Results	2
1.3 Discussion of Results	5
1.4 Conclusions	18
References	19
CHAPTER 2 - FINITE ELEMENT SIMULATION OF BRAZILIAN TEST	20
2.1 Introduction	20
2.2 Formulation of Essential Matrices for Three-Dimensional Elements	20
2.3 Formulation of Essential Matrices for Two-Dimensional Elements	33
2.4 Failure Criteria	38
2.5 Concluding Remarks	41
References	42
CHAPTER 3 - TWO-DIMENSIONAL PROGRAM	43
3.1 Introduction	43
3.2 Description of Program	43
3.3 Test Problems	44
3.4 Discussion of Results	52
3.5 Conclusions	52
References	58
APPENDIX A - TWO-DIMENSIONAL PROGRAM LISTING	59

LIST OF FIGURES

FIGURE 1.1	The MB Universal Testing Machine	3
FIGURE 1.2	Brazilian Test	4
FIGURE 1.3	Strength vs. Length, Dacite, Strain Control	6
FIGURE 1.4	Strength vs. Diameter, Dacite, Strain Control	7
FIGURE 1.5	Strength vs. Length, Dacite, Stress Control	8
FIGURE 1.6	Strength vs. Diameter, Dacite, Stress Control	9
FIGURE 1.7	Strength vs. Length, Valders Limestone, Strain Control	10
FIGURE 1.8	Strength vs. Length, Valders Limestone, Stress Control	11
FIGURE 1.9	Strength vs. Diameter, Valders Limestone, Strain Control	12
FIGURE 1.10	Strength vs. Diameter, Valders Limestone, Stress Control	13
FIGURE 1.11	Strength vs. Length, St. Cloud Gray Granodiorite, Strain Control	14
FIGURE 1.12	Strength vs. Length, St. Cloud Gray Granodiorite, Stress Control	15
FIGURE 1.13	Strength vs. Diameter, St. Cloud Gray Granodiorite, Strain Control	16
FIGURE 1.14	Strength vs. Diameter, St. Cloud Gray Granodiorite, Stress Control	17
FIGURE 2.1	Materials Properties Considered in Analysis	21
FIGURE 2.2	Element Models with Local Node Numbers Indicated	23
FIGURE 2.3	Relationship Between Global and Local Coordinates	24
FIGURE 2.4	Step-by-Step Orientation of Axes of Anisotropy	30
FIGURE 2.5	Positive Direction of Stresses and Displacements	31
FIGURE 2.6	Stress Tetrahedron.	35
FIGURE 2.7	Nodal Coordinates of Three-Dimensional Element	36
FIGURE 2.8	Stress Cube.	40

FIGURE 3.1	Standard Scheme for Numbering Nodes and Elements of Two-Dimensional Disc46
FIGURE 3.2	Flow Chart of Two-Dimensional Program47
FIGURE 3.3	Stress Distribution Along Line of Diametral Load (Test Problem No. 1)48
FIGURE 3.4	Finite Element Mesh for Problem 2 and 349
FIGURE 3.5	Progression of Failure in Test Problem No. 254
FIGURE 3.6	Progression of Failure in Test Problem No. 355
FIGURE 3.7	Load-Displacement Curve (Homogeneous Case)56
FIGURE 3.8	Load-Displacement Curve (Nonhomogeneous Case)57

LIST OF TABLES

TABLE 2.1	The Matrix [c]	28
TABLE 2.2	The Matrix [q]	29
TABLE 2.3	The Transformation Matrix [T]	34

PART A

**ASPECTS OF MECHANICAL BEHAVIOR OF ROCK
UNDER STATIC AND CYCLIC LOADING**

**A FINITE ELEMENT MODEL OF ROCK FAILURE
FROM THE BRAZILIAN TEST**

**Jesus Basas
A. Hayatdavoudi
Robert W. Heins**

September 1972

**Department of Metallurgical & Mineral Engineering
The University of Wisconsin
Madison, Wisconsin 53706**

Vii

CHAPTER 1

SIZE EFFECT ON BRAZILIAN TEST

1.1 Introduction

When applying values of mechanical properties of rocks obtained from laboratory tests to actual problems, it is essential for reasons of safety and economy that size effect, if any, be established. A design, for example, that does not take into account size effect could be unsafe if, in fact, size effect exists. On the other hand, a design based on the existence of size effect could be overly conservative if no such effect exists.

Although considerable experimental work has been undertaken to determine size effect in rocks, the findings have so far been inconclusive and often contradictory. In tests to study size-strength dependence, it has been observed (2) that, with increasing size, strength either (a) decreases, (b) remains unchanged, or (c) increases. A very logical explanation of these widely divergent size effects was offered by Koifman (3). He hypothesized that size effect is governed by two factors, namely: natural internal imperfections which he called "volume" factor and "changes in the surface layers, brought about by mechanical, physical or chemical action, or by influences of the environment" which he called "surface" factor. Koifman claimed that with increased size, strength will decrease when the "volume" factor is dominant, could increase if the "surface" factor is dominant, or will remain the same if the two factors balance each other. He went on to say that under tensile stresses the "volume" factor will always prevail and hence, the strength of the rock will always decrease with increasing size. He based his argument on the assumption that the number and extent of the internal flaws increases with size. Although this assumption has a statistical basis, it might not be valid in actual situations.

Indeed, in rock masses where nonhomogeneity occurs more often than not a sample taken from a relatively defect-free region could easily contain much fewer structural defects than smaller samples taken from other regions not quite as defect-free. This is particularly true for small-size samples such as those used in laboratory tests. Furthermore, in Brazilian tests the tensile strength could be much more sensitive to the position and orientation of the structural defects relative to the loading axis than the number and extent of these defects. Thus, in Brazilian tests at least, the possibility of strength increasing with size should not be ruled out. Several investigators (2, 3) have reported such a size-strength variation.

In the present study, an attempt will be made to correlate specimen size and tensile strength as obtained from Brazilian test. Three types of rocks were tested. These are Valders limestone, St. Cloud gray granodiorite, and dacite.

1.2 Experimental Procedure and Results

The tests were carried out on a MB Universal Testing Machine (Fig. 1.1) according to the procedure described in the first annual progress report (1). The specimens were 1", 2" and 3" in diameter and 1/2", 1" and 2" in length (or thickness), with all nine possible combinations of length and diameter represented. The specimens were tested in random order and without due regard as to which diametral axis would be loaded. At least three samples of each size were tested. A typical Brazilian test set-up is shown in Fig. 1.2.

Two modes of testing, namely, stress-controlled mode and strain-controlled mode, were used. In the stress-controlled mode, the load is applied at a predetermined constant rate of approximately 100 pounds per second. In the strain-controlled mode, the load is applied at a varying rate depending on the lateral strain at the center of the specimen. In the latter mode the load can be reduced faster than the specimen breaks thus avoiding the catastrophic failure which characterizes stress-controlled tests.

Reproduced from
best available copy.

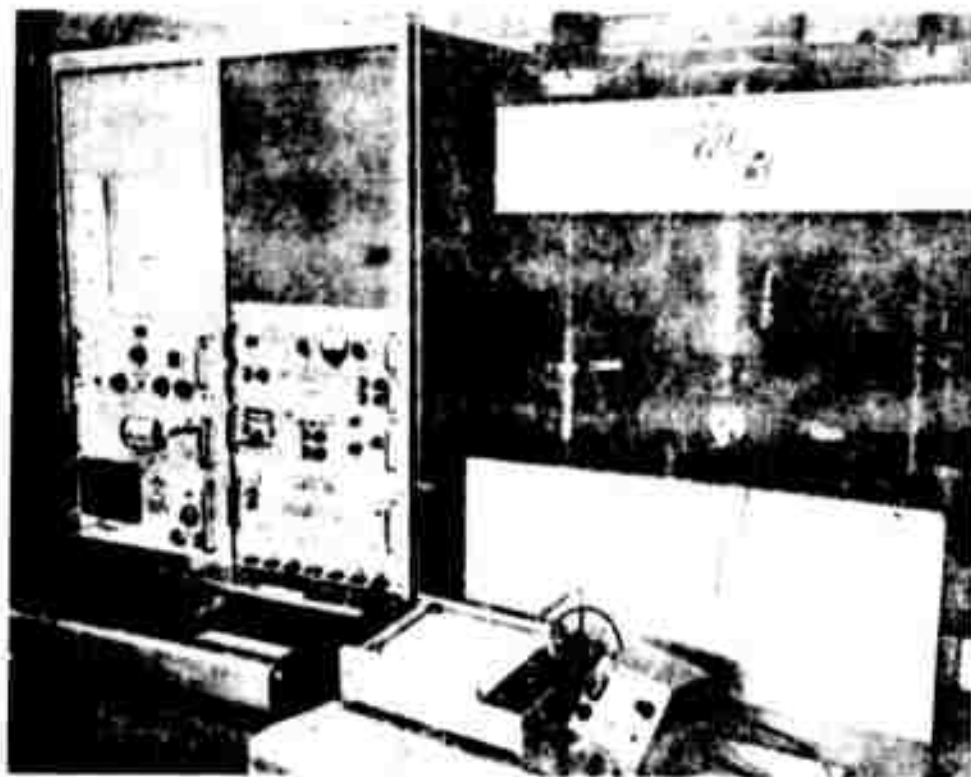
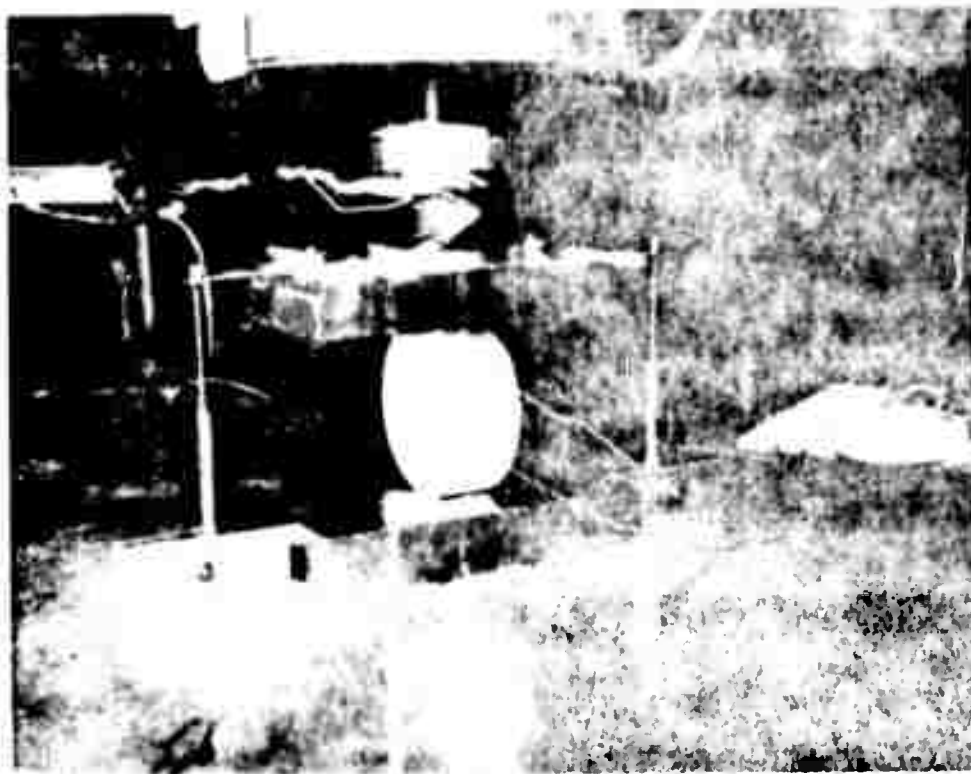


Figure 1.1 The MB Universal Testing Machine



Reproduced from
best available copy.

Figure 1.2 Brazhlin Test

It is thus possible to obtain complete stress-strain curves in strain-controlled tests.

To make the two loading modes equivalent during the early stage of loading, the strain-controlled mode was programmed to provide a maximum strain of 10,000 micro-inch per inch in 800 seconds. This rate, it was estimated, is approximately equal to the 100 lbs./sec. rate used in the stress-controlled mode.

Plots of tensile strength (σ_t) versus specimen dimensions for all rocks are shown in Figs. 1.3 through 1.14. The curves were plotted on the basis of the equation,

$$\sigma_t = \theta_1 L^{\theta_2} D^{\theta_3}$$

in which L is length; D is diameter; and θ_1 , θ_2 , and θ_3 are constant parameters. The values of the constant parameters corresponding to the condition of "best fit" can be obtained by means of a statistical procedure called regression analysis (5).

1.3 Discussion of Results

All kinds of strength-size variation are shown in the plots. In the harder rocks (St. Cloud gray granodiorite and Valders limestone in some cases) there appears to be a definite correlation between size and strength. Some agree with Koifman's prediction. The apparent absence of definite pattern of the size-strength relationship in the other plots could be attributed to one or a combination of the following:

- (a) The size differences between the specimens were not large enough.
- (b) Not enough samples were tested for certain sizes particularly in strain-controlled tests.
- (c) Valders limestone and dacite are not nearly homogenous and isotropic as first thought. The tensile strength was, therefore, affected more by the position and orientation

DACITE STRAIN CONTROL

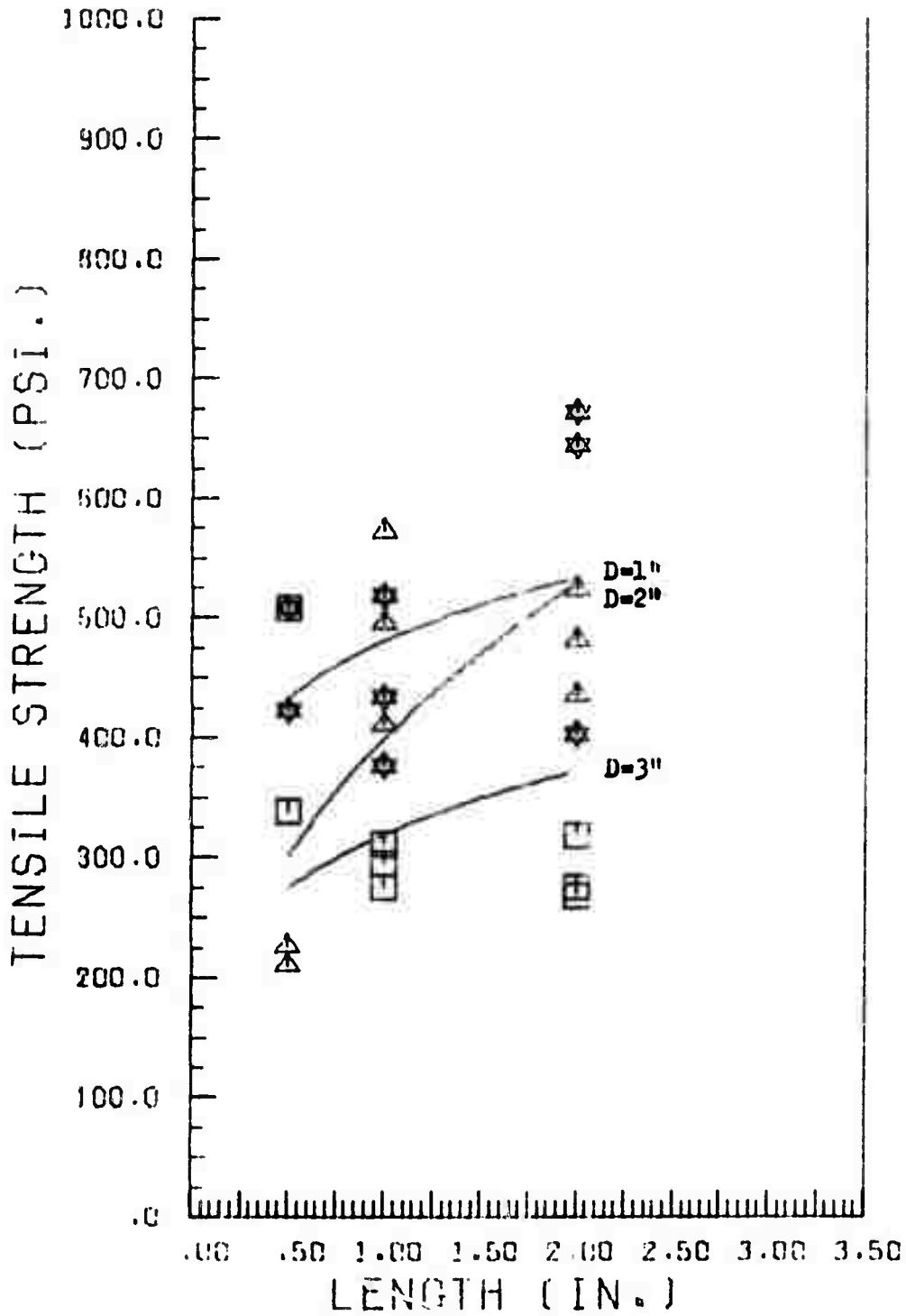


Figure 1.3

DACITE STRAIN CONTROL

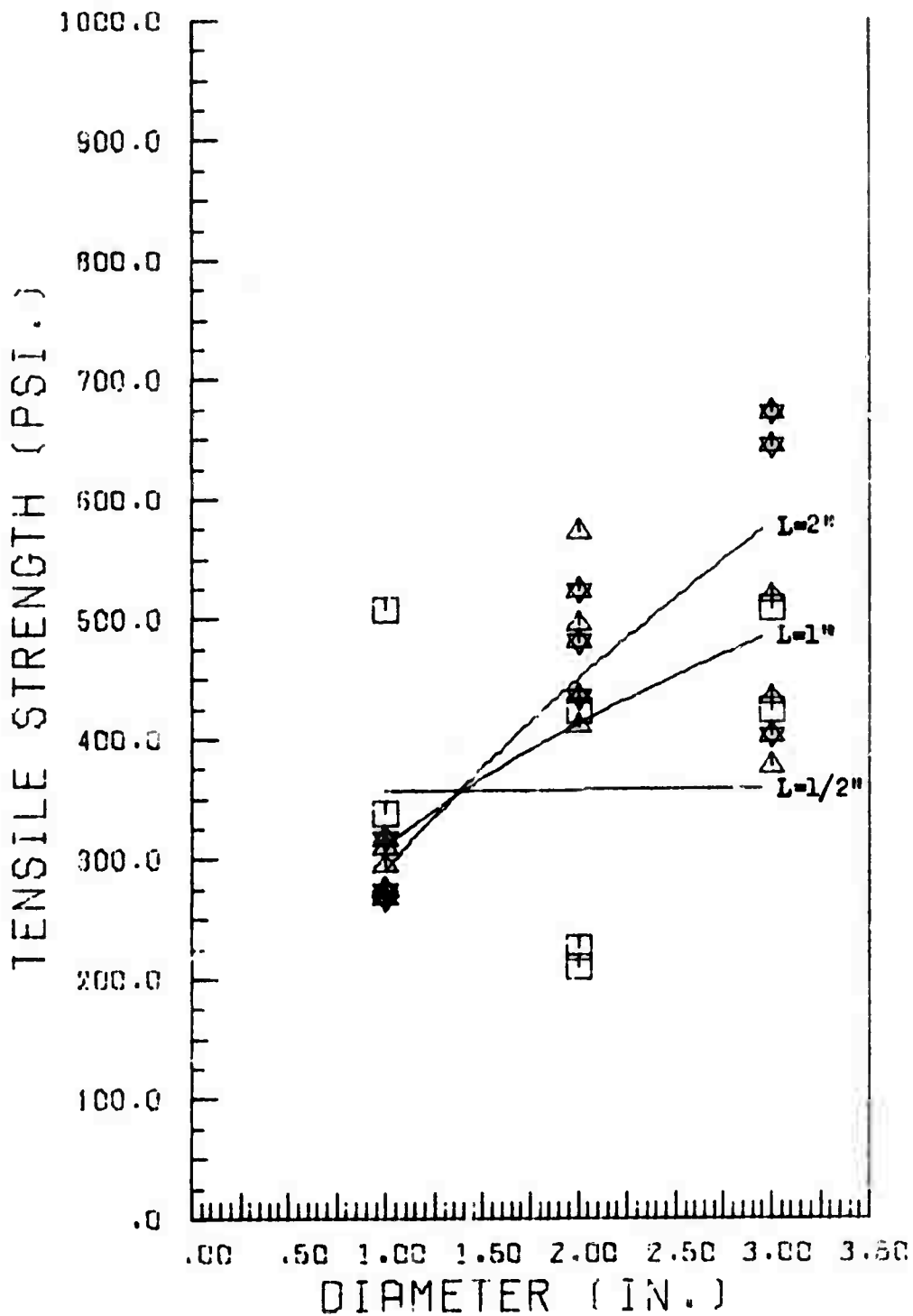


Figure 1.4

DACITE STRESS CONTROL

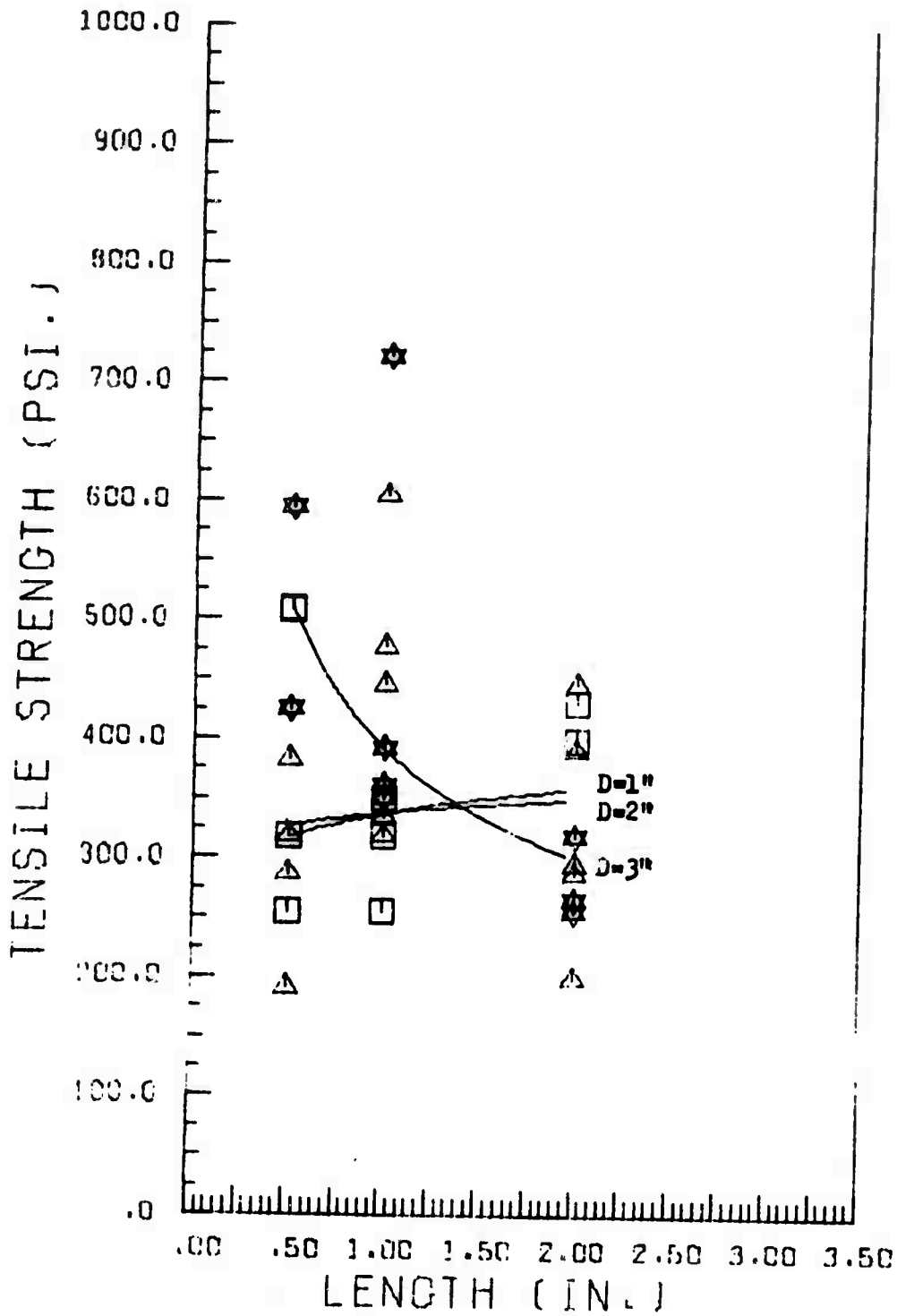


Figure 1.5

DACITE STRESS CONTROL

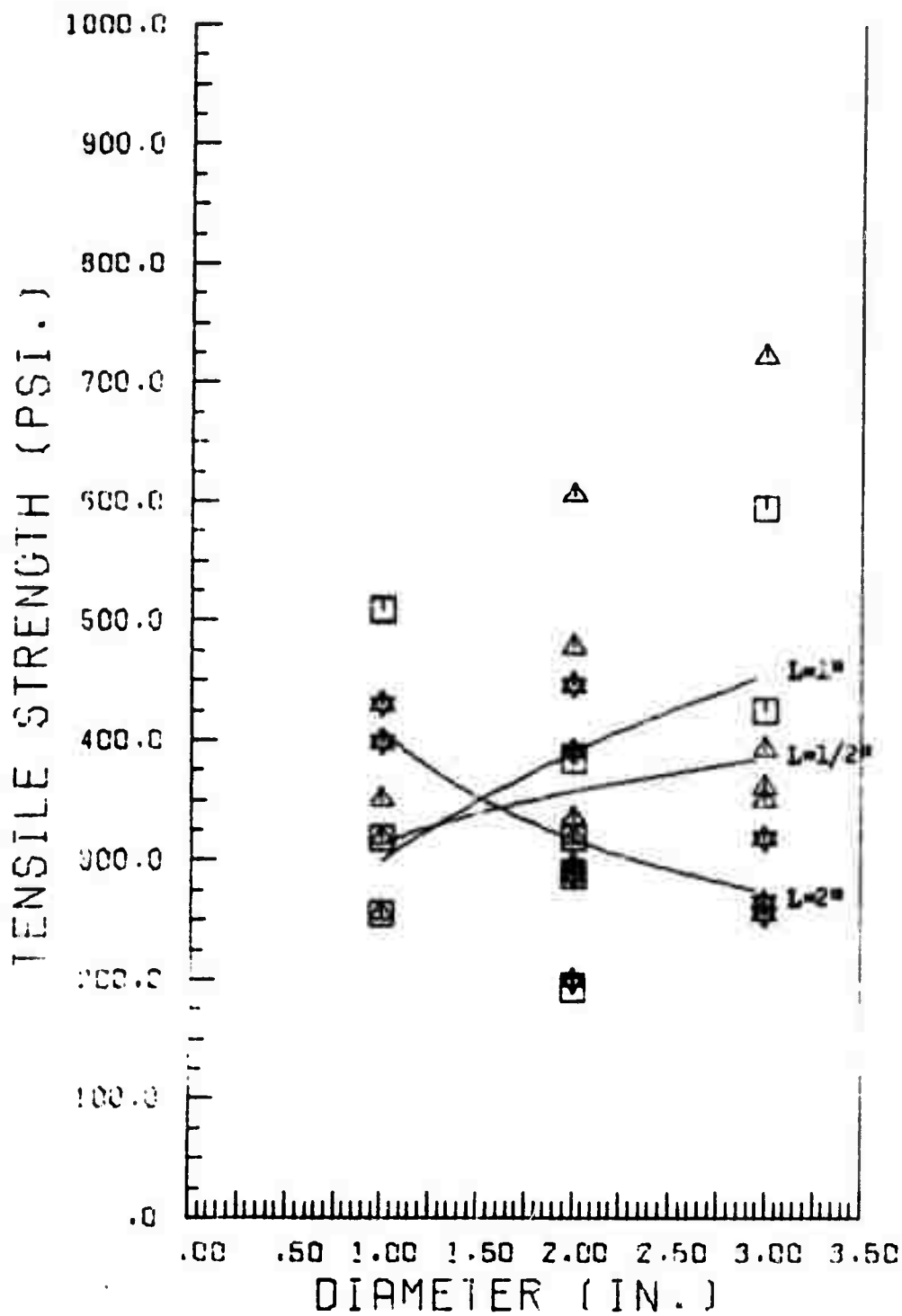


Figure 1.6

VALDERS LIMESTONE STRAIN CONTROL

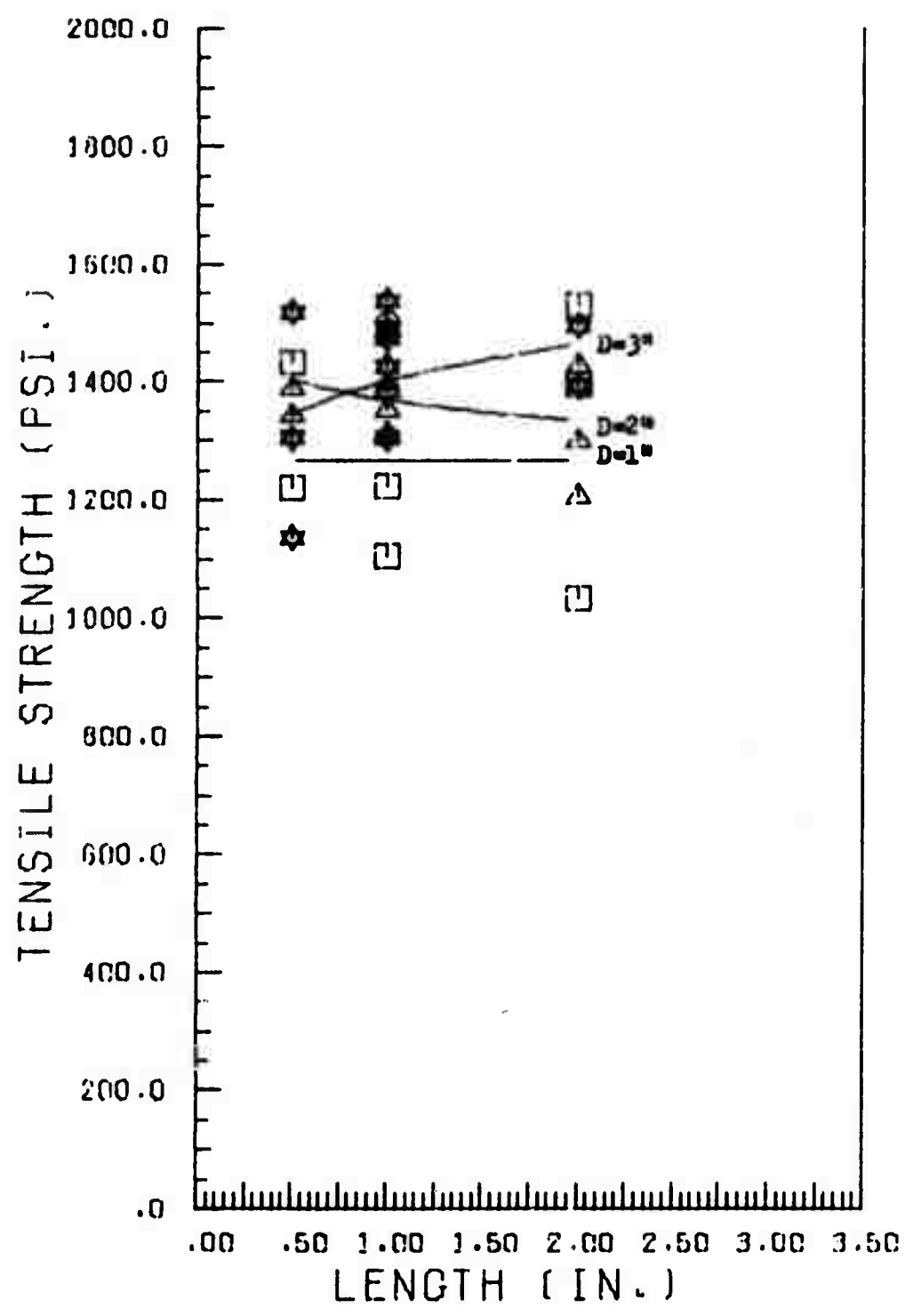


Figure 1.7

VALDERS LIMESTONE STRESS CONTROL

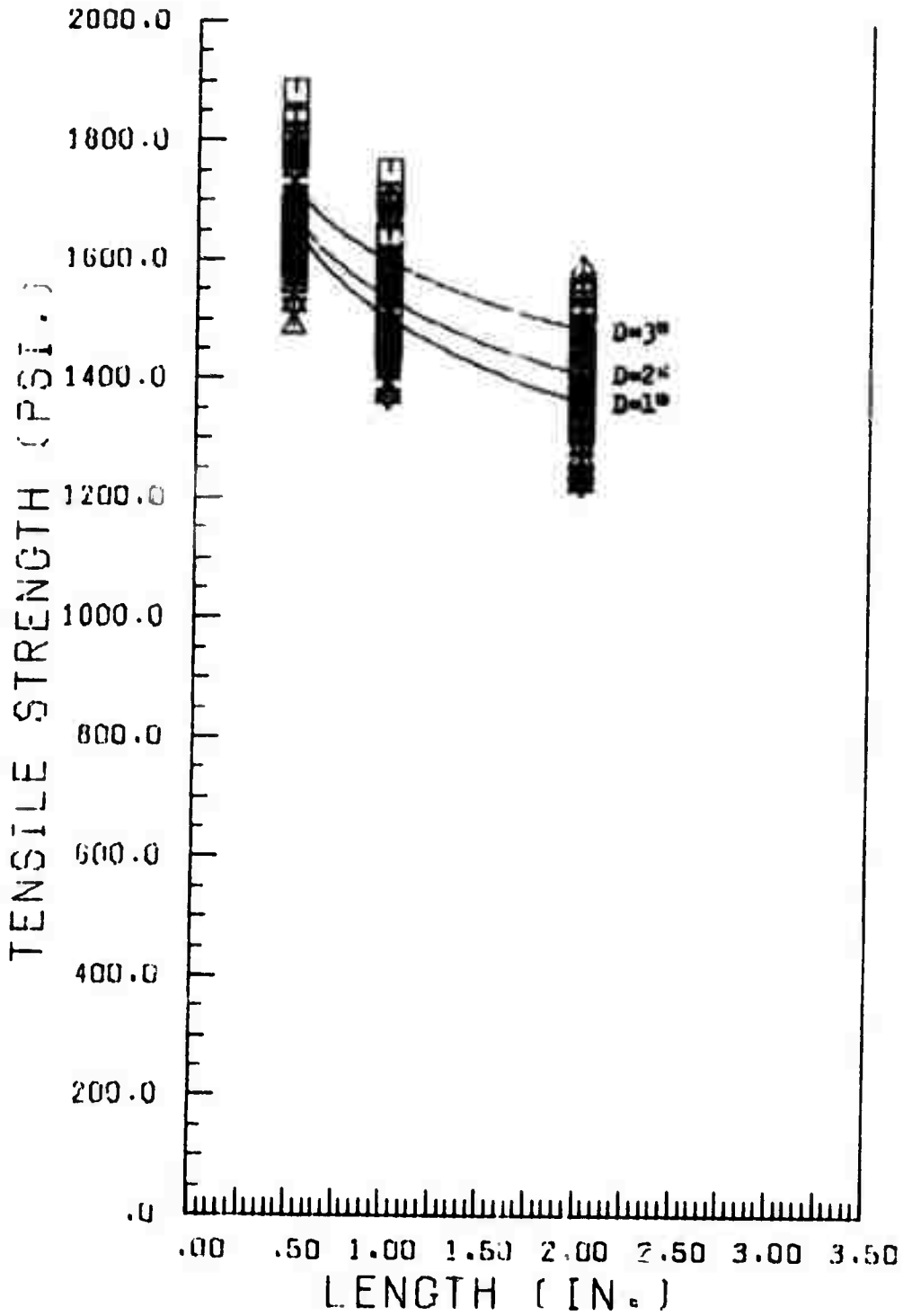


Figure 1.8

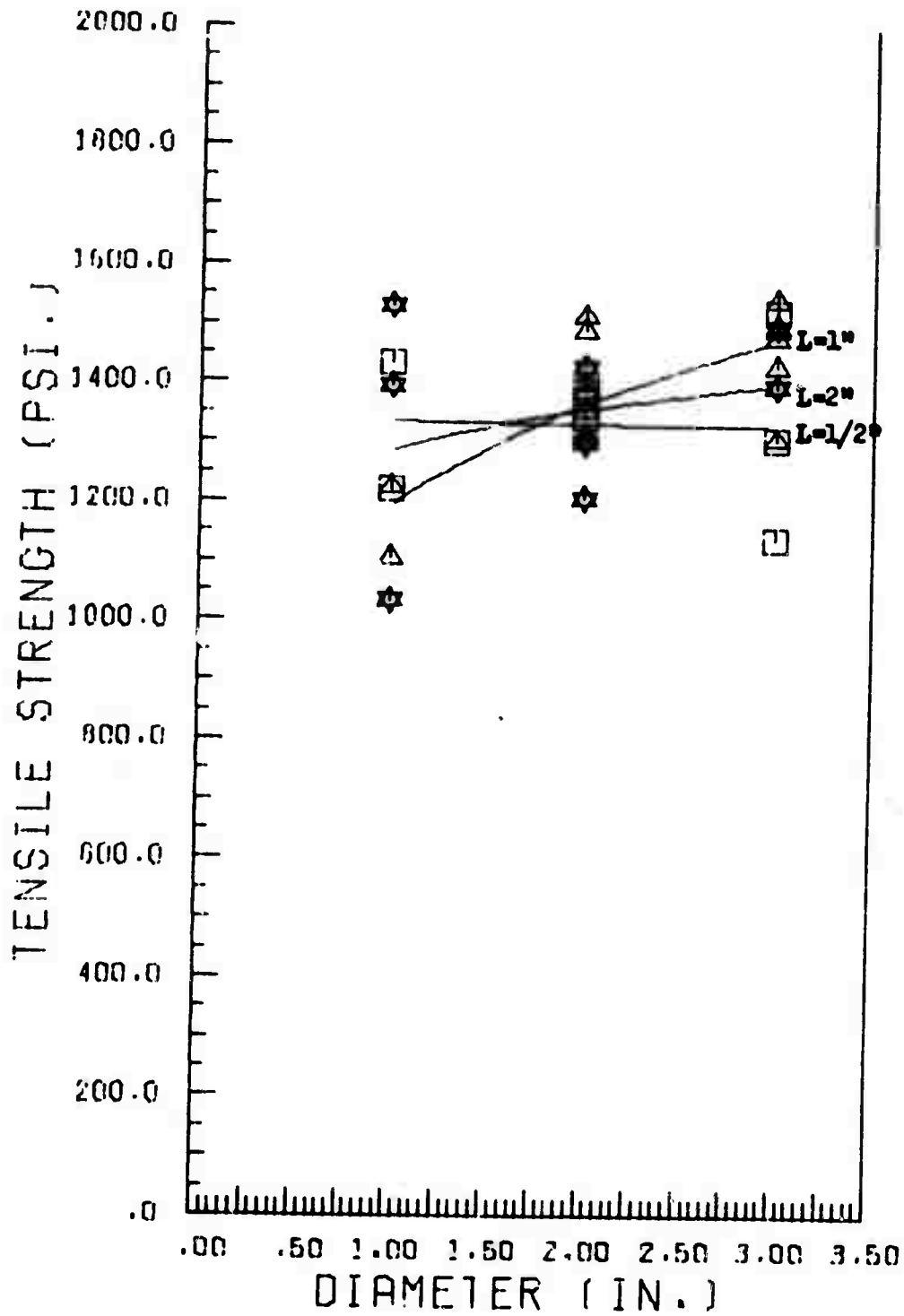
VALDEFS LIMESTONE
STRAIN CONTROL

Figure 1.9

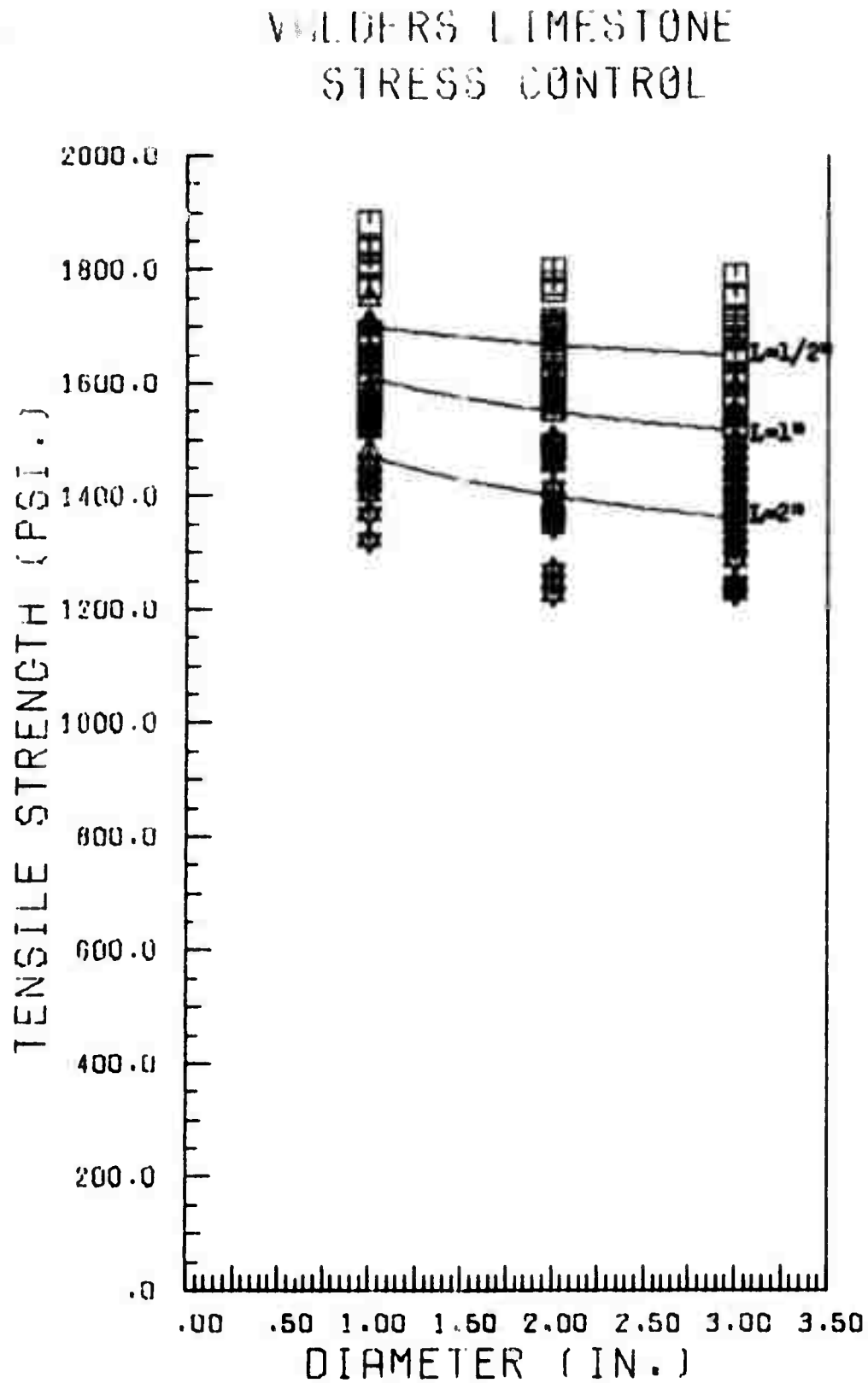


Figure 1.10

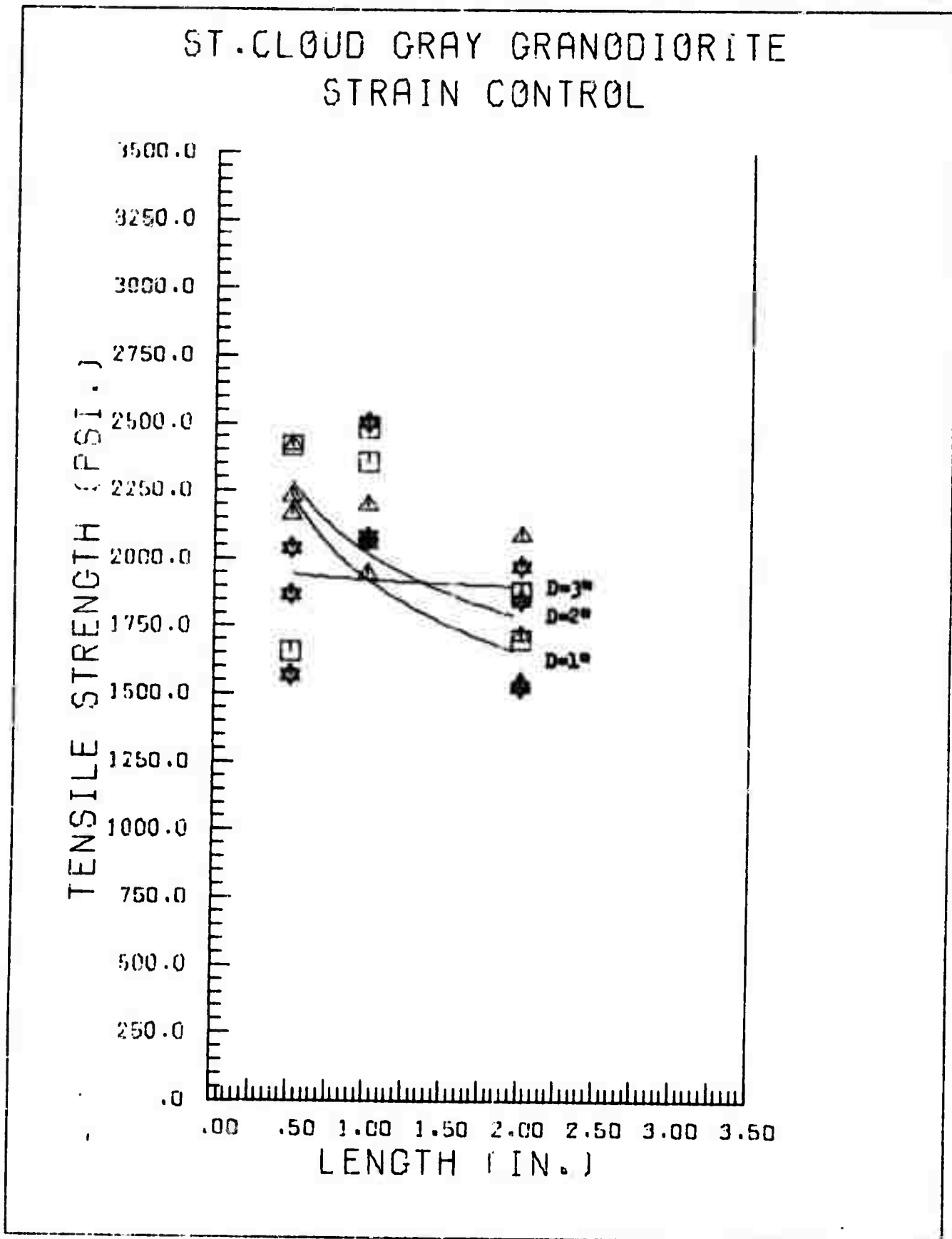


Figure 1.11

ST. CLOUD GRAY GRANODIORITE STRESS CONTROL

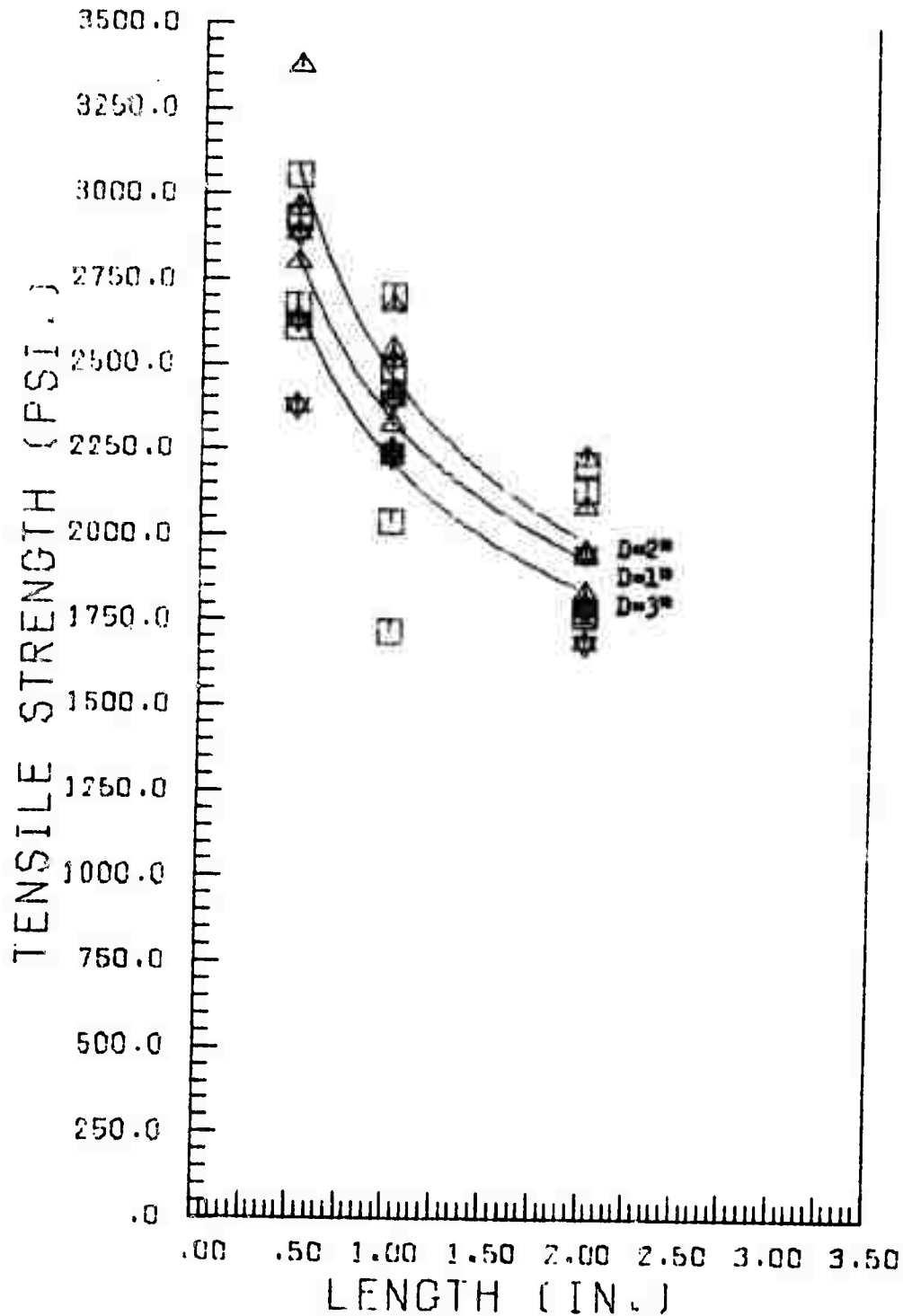


Figure 1.12

ST. CLOUD GRAY GRANODIORITE STRAIN CONTROL

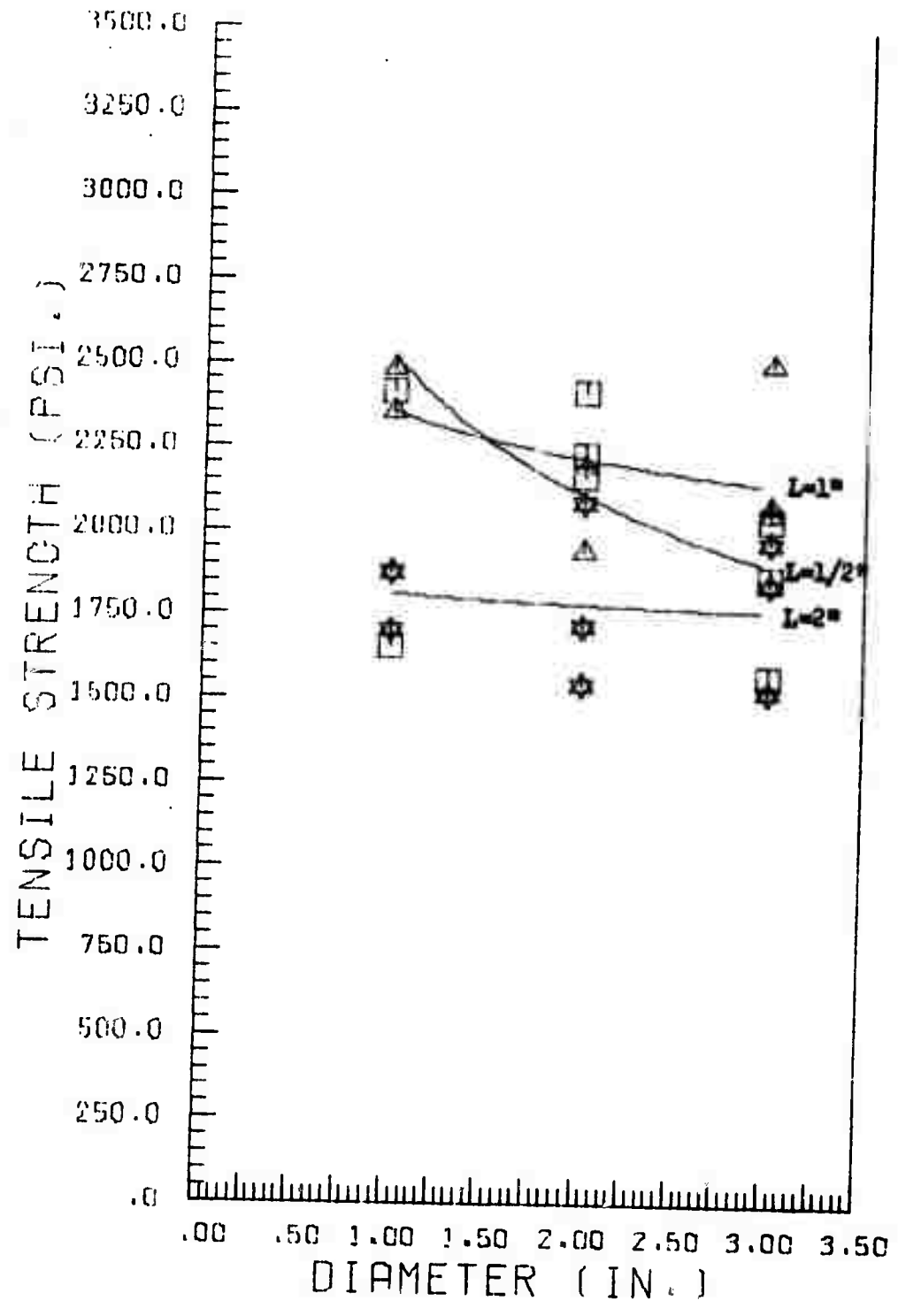


Figure 1.13

ST. CLOUD GRAY GRANODIORITE STRESS CONTROL

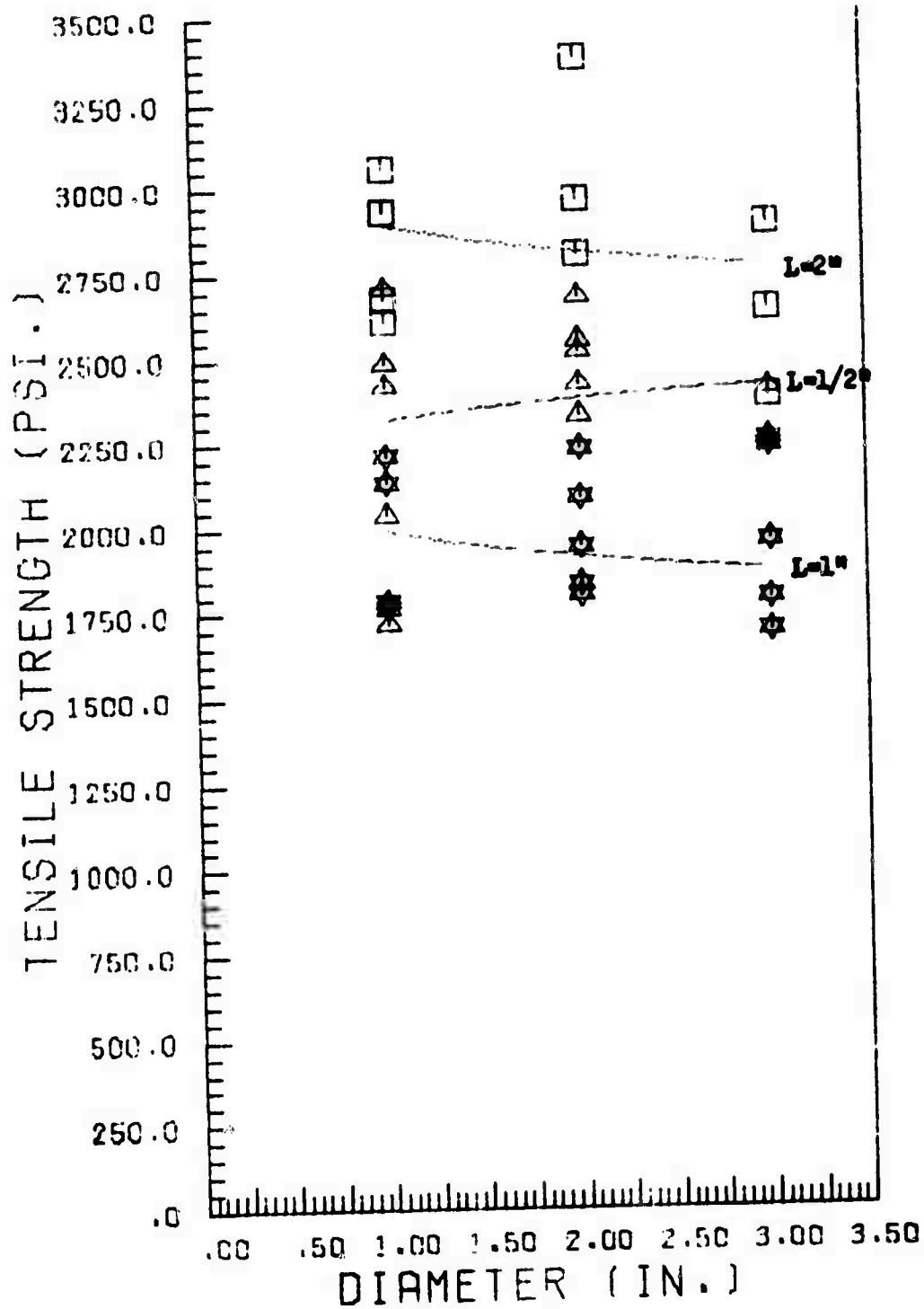


Figure 1.14

of the internal structural defects with respect to the loaded diametral plane than by the number and extent of said defects. This also explains the scattering of the data points.

1.4 Conclusions

There is definitely a size effect on tensile strength. In Brazilian tests, the size effect will be governed mainly by the position and orientation of the internal defects relative to the loaded diametral plane rather than by the extent and number of the defects. For this reason, the Brazilian test is not a good basis for studying size-tensile strength dependence unless care is taken to consistently load the specimens along the same diametral plane. The splitting test described by Koifman (6) appears to be a better alternative.

The size difference between the specimens used in this study was not large enough to predict a definite pattern of size-strength relationship especially in the case of the soft rocks. Future tests should include larger specimens.

REFERENCES

1. Heins, R. W., et al, "Aspects of Mechanical Behavior of Rock Under Static and Cyclic Loading (Part A: Mechanic Behavior of Rock Under Static Loading)", First Annual Progress Report, Engineering Experiment Station, University of Wisconsin, Madison, Wisconsin, March 1972.
2. Brown, E. T., "Strength-Size Effect in Rock Material", Progress Report No. 24, University of Minnesota Mineral Resources Center, April 1971.
3. Koifman, M. I., "The Size Factor in Rock Pressure Investigations", Mechanical Properties of Rocks by M. M. Protod'yakonov, M. I. Koifman, and others, Moscow Acad. Sci., USSR (translated by Israel Prog. Sci. Trans., Jerusalem), 1963.
4. Jaeger, J. C. and N. G. W. Cook, Fundamentals of Rock Mechanics, Methuen & Co., Ltd., London, 1969.
5. Draper, N. R. and H. Smith, Applied Regression Analysis, John Wiley and Sons, Inc., New York, 1966.
6. Koifman, M. I., "Quick Combined Method of Determining Mechanical Properties of Rocks", Mechanical Properties of Rocks by M. M. Protod'yakonov, M. I. Koifman, and others, Moscow Acad. Sci., USSR (translated by Israel Prog. Sci. Trans., Jerusalem), 1963.

CHAPTER 2

FINITE ELEMENT SIMULATION OF BRAZILIAN TEST

2.1 Introduction

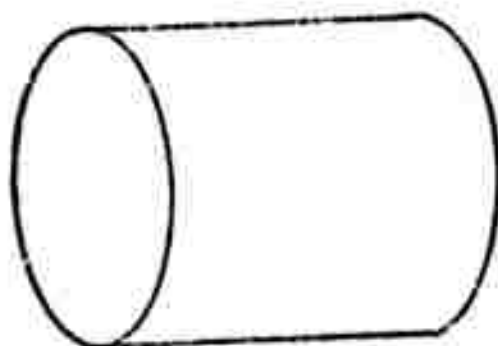
A theoretical version of the Brazilian test employing the finite element technique is described in this chapter. In connection with the proposed method, development of a highly efficient computer program which will be based on both three-dimensional and two-dimensional elements and which will account for material anisotropy as well as nonhomogeneity is now underway. A two-dimensional program which takes into account nonhomogeneity but not anisotropy has already been developed and will be described in the next chapter.

In the treatment of nonhomogeneous problems, the basic idea suggested in the first annual report will be used; that is, elastic properties will be assigned randomly to each element by means of a random number generating routine. Other failure criteria not touched in the first annual report will be investigated. It has been experimentally demonstrated (1) that although rock is essentially a brittle material, it attains an unusually high degree of ductility when subjected to high confining pressures. This phenomenon, however, is vaguely defined in literature and will, therefore, be taken into account only approximately when considering post-failure behavior of elements.

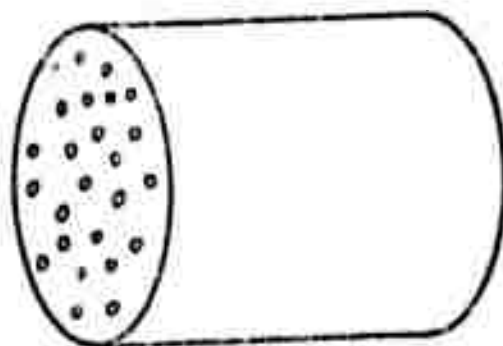
In writing this report, it is assumed that the reader is familiar with the basic principles of matrix algebra and the finite element method. No attempt will be made to rederive equations which have already been derived in previous publications.

2.2 Formulation of Essential Matrices for Three-Dimensional Elements

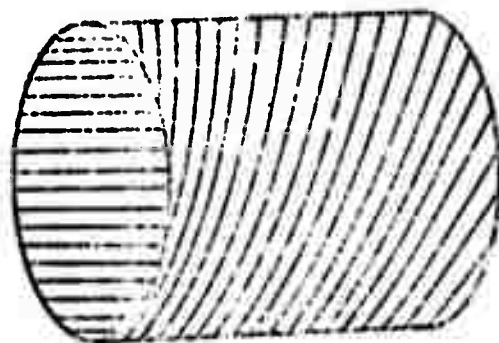
In the finite element method of analysis, the whole structural system is idealized as an assemblage of elements which are connected to one another only at a discrete number of nodal points. The nodal displacements are the



(a) Homogeneous and isotropic



(b) Nonhomogeneous



(c) Homogeneous and anisotropic

FIGURE 2.1 Material Properties Considered in Analysis

basic unknown quantities of the method upon which the displacement pattern and therefore the stresses within the boundaries of the element depend. To facilitate the calculation of the element stiffness properties, a set of displacement functions, usually polynomials, are assumed. These functions uniquely define the deformations allowed within an element in terms of the nodal displacements.

In this study, the Brazilian test specimen is divided by imaginary annular surfaces and radial planes into elements of the kind shown in Fig. 2. 2. The corner points of the elements are designated as the nodal points. Eight-term linear polynomials are used to represent the radial (u), circumferential (v), and axial (w) displacements within an element. Thus

$$\begin{Bmatrix} u \\ v \\ w \end{Bmatrix} = \begin{bmatrix} 1 & r' & \theta' & r'\theta' & z' & r'z' & \theta'z' & r'\theta'z' & 0 & 0 & 0 & 0 \\ 0 & 0 & 0 & 0 & 0 & 0 & 0 & 0 & 1 & r' & \theta' & r'\theta' \\ 0 & 0 & 0 & 0 & 0 & 0 & 0 & 0 & 0 & 0 & 0 & 0 \\ 0 & 0 & 0 & 0 & 0 & 0 & 0 & 0 & 0 & 0 & 0 & 0 \\ z' & r'z' & \theta'z' & r'\theta'z' & 0 & 0 & 0 & 0 & 0 & 0 & 0 & 0 \\ 0 & 0 & 0 & 0 & 1 & r' & \theta' & r'\theta' & z' & r'z' & \theta'z' & r'\theta'z' \end{bmatrix} \begin{Bmatrix} a_1 \\ a_2 \\ a_3 \\ \vdots \\ a_{24} \end{Bmatrix} \tag{2. 1}$$

where a_1, a_2, \dots, a_{24} are the constant coefficients of the polynomials and (r', θ', z') are local dimensionless cylindrical coordinates which range in value from -1 to +1 within an element. The global cylindrical coordinates (r, θ, z) are related to the local coordinates as follows:

$$\begin{aligned} r &= r_o + r_s r' \\ \theta &= \theta_o + \theta_s \theta' \\ z &= z_o + z_s z' \end{aligned} \tag{2. 2}$$

where (r_o, θ_o, z_o) are the global coordinates of the origin of the local coordinate axes and $2r_s, 2\theta_s$ and $2z_s$ are the side dimensions of the element (see Fig. 2. 3).

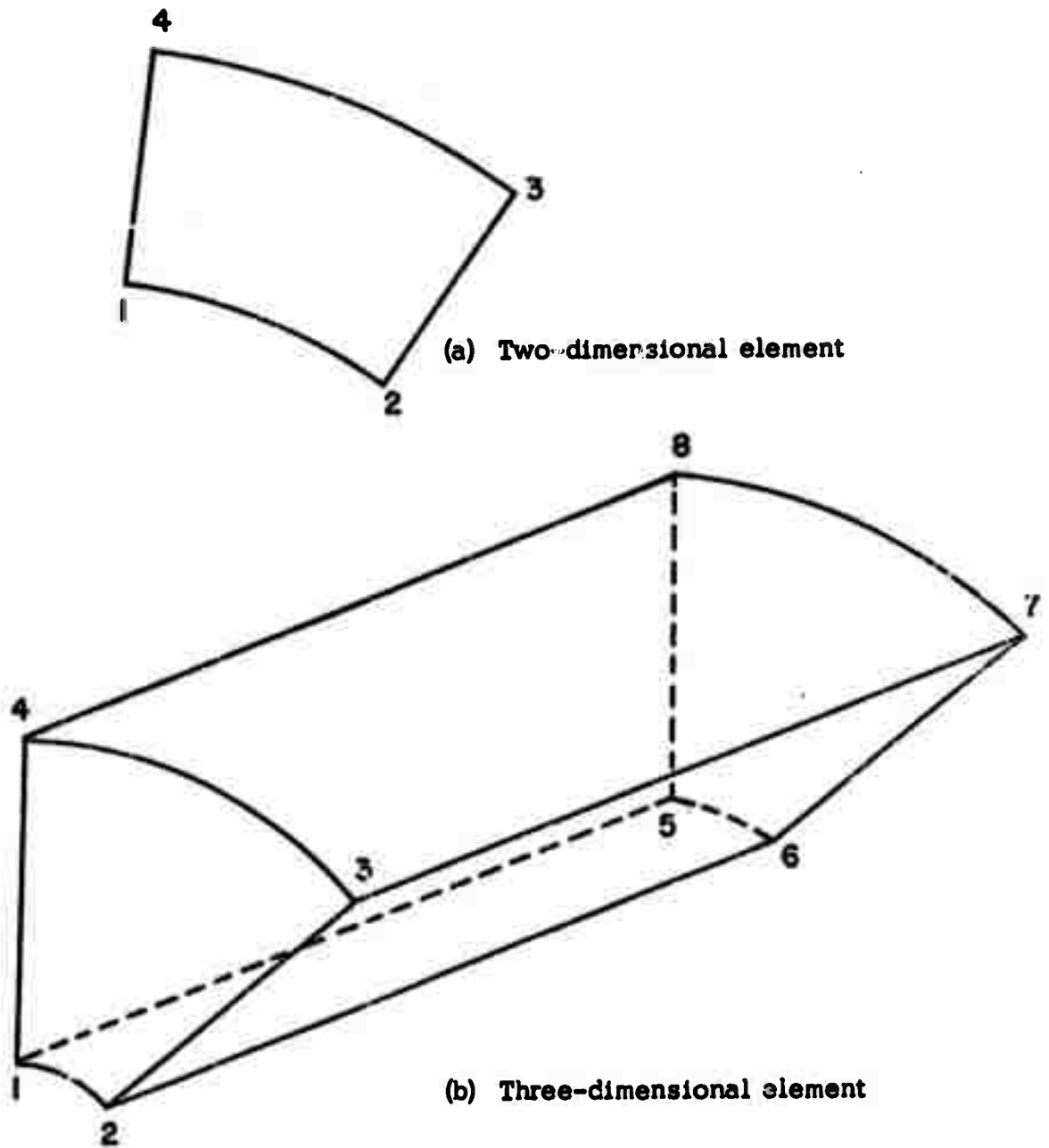


FIGURE 2.2 Element Models With Local Node Numbers Indicated

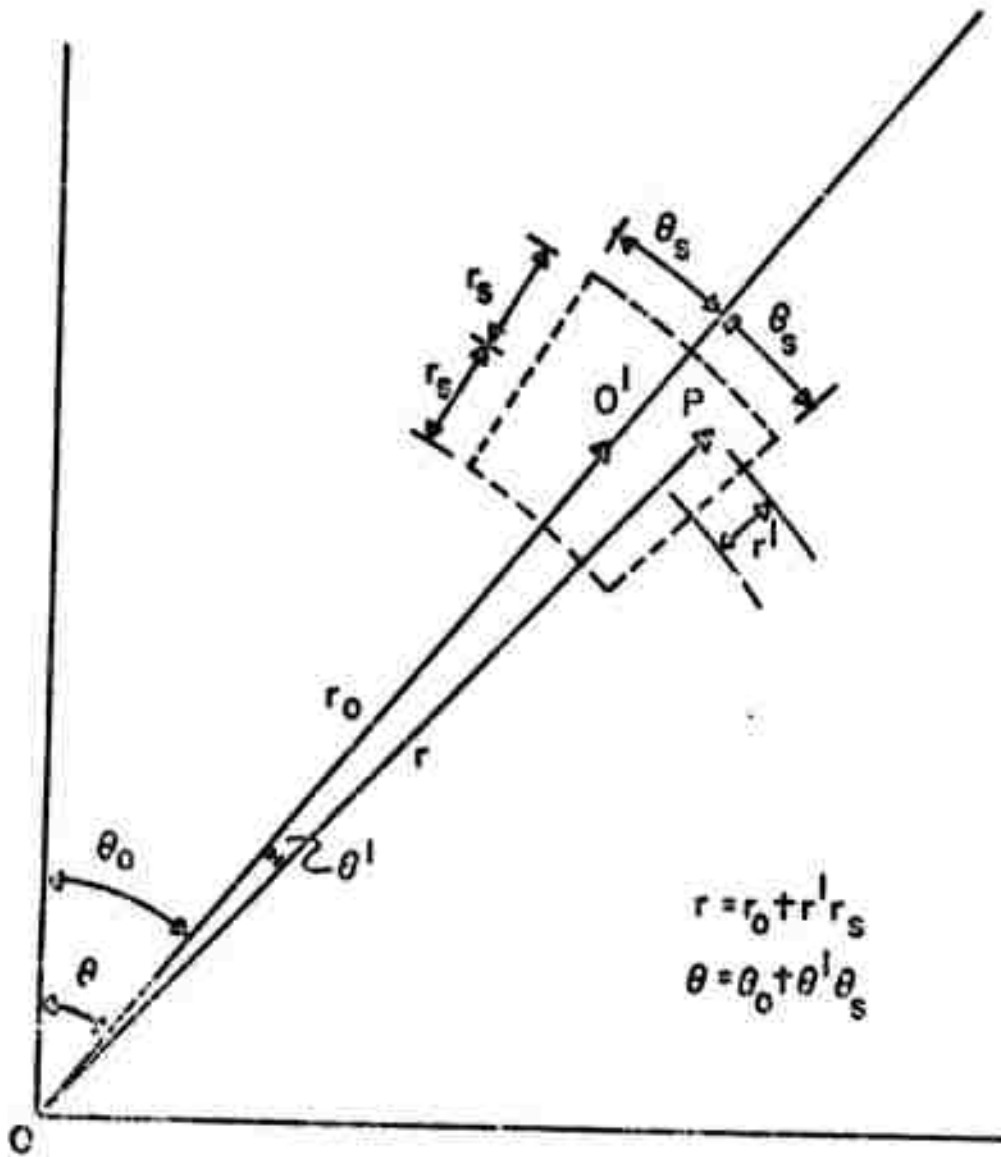


FIGURE 2.3 Relationship Between Global and Local Coordinates

To obtain the displacements at any node i , one merely substitutes into eq. (2. 1) the appropriate nodal coordinates, that is,

$$\begin{aligned} u_i &= a_1 + a_2 r'_i + a_3 \theta'_i + a_4 r'_i \theta'_i + \dots \\ v_i &= a_9 + a_{10} r'_i + a_{11} \theta'_i + a_{12} r'_i \theta'_i + \dots \\ w_i &= a_{17} + a_{18} r'_i + a_{19} \theta'_i + a_{20} r'_i \theta'_i + \dots \end{aligned} \quad (2. 3)$$

where r'_i , θ'_i , z'_i are equal to +1 or -1. Thus, if $\{x\}^*$ denotes the nodal displacement vector $\{u_1 \ v_1 \ w_1 \ u_2 \ v_2 \ \dots \ v_8 \ w_8\}$ and $\{a\}$ the constant coefficient array, then

$$\{x\} = [c] \{a\} \quad (2. 4)$$

The matrix $[c]$ is shown in Table 2. 1. It can easily be verified that

$$[c]^{-1} = \frac{1}{8} [c]^T \quad (2. 5)$$

From the equations for the components of strain at a point,

$$\{\epsilon\} = \begin{Bmatrix} \epsilon_r \\ \epsilon_\theta \\ \epsilon_z \\ \gamma_{r\theta} \\ \gamma_{rz} \\ \gamma_{\theta z} \end{Bmatrix} = \begin{Bmatrix} \frac{\partial u}{\partial r} \\ \frac{u}{r} + \frac{\partial v}{r \partial \theta} \\ \frac{\partial w}{\partial z} \\ \frac{\partial u}{r \partial \theta} + \frac{\partial v}{\partial r} - \frac{v}{r} \\ \frac{\partial u}{\partial z} + \frac{\partial w}{\partial r} \\ \frac{\partial v}{\partial z} + \frac{\partial w}{r \partial \theta} \end{Bmatrix} \quad (2. 6)$$

one obtains, with the aid of eqs. (2. 1) and (2. 2), the relationship

$$\{\epsilon\} = [q] \{a\} \quad (2. 7)$$

where the elements of $[q]$ are listed in Table 2. 2.

The stress components are related to the strain components by the elasticity matrix $[D]$, that is

$$\{\sigma\} = [D] \{\epsilon\} \quad (2. 8)$$

where, for the isotropic case

* The symbol $\{ \}$ denotes column matrices while $[\]$ denotes all other matrices.

$$[D] = \begin{bmatrix} \frac{(1-\nu)E}{(1+\nu)(1-2\nu)} & \frac{\nu E}{(1+\nu)(1-2\nu)} & \frac{\nu E}{(1+\nu)(1-2\nu)} & 0 & 0 & 0 \\ & \frac{(1-\nu)E}{(1+\nu)(1-2\nu)} & \frac{\nu E}{(1+\nu)(1-2\nu)} & 0 & 0 & 0 \\ & & \frac{(1-\nu)E}{(1+\nu)(1-2\nu)} & 0 & 0 & 0 \\ \text{Symmetric} & & & G & 0 & 0 \\ & & & & G & 0 \\ & & & & & G \end{bmatrix}$$

E = modulus of elasticity

ν = Poisson's ratio

G = shear modulus = $\frac{E}{2(1+\nu)}$

and

$$(\sigma) = \{\sigma_r \quad \sigma_\theta \quad \sigma_z \quad \tau_{r\theta} \quad \tau_{rz} \quad \tau_{\theta z}\} \quad (\text{see Fig. 2.5})$$

The formulation of $[D]$ for the case where the material is anisotropic requires added consideration. Let 1, 2, 3 be the axes of anisotropy (assumed mutually perpendicular) and $\alpha_1, \alpha_2, \alpha_3$ the angles which define the orientation of these axes. To understand more clearly the significance of the parameters $\alpha_1, \alpha_2, \alpha_3$, a step-by-step rotation of the axes 1, 2, 3 to their actual positions is illustrated in Fig. 2.4. Let axes 2, 3 lie in the plane ABCD. In Fig. 2.4a, axis 3 and plane ABCD are initially positioned parallel to the Z-axis of the element, α_1 being the angle which plane ABCD makes with the radial plane passing through the central point of the element. In Fig. 2.4b, plane ABCD is rotated an angle α_2 about axis 2 to A'B'C'D'. Figure 2.4c shows the actual orientation of axes 1, 2, 3 arrived at by rotating axes 2, 3 an angle α_3 in their own plane (A'B'C'D'). It should be noted that if material properties do not vary in the plane of 2, 3, then α_3 can be arbitrarily set to any value, say zero.

The stress-strain relations for general anisotropy are given in the theory of elasticity as

$$\begin{aligned}
 \epsilon_1 &= \frac{\sigma_1}{E_1} - \frac{\nu_{12}\sigma_2}{E_2} - \frac{\nu_{13}\sigma_3}{E_3} \\
 \epsilon_2 &= -\frac{\nu_{12}\sigma_1}{E_2} + \frac{\sigma_2}{E_2} - \frac{\nu_{23}\sigma_3}{E_3} \\
 \epsilon_3 &= -\frac{\nu_{13}\sigma_1}{E_3} - \frac{\nu_{23}\sigma_2}{E_3} + \frac{\sigma_3}{E_3} \\
 \gamma_{12} &= \frac{1}{G_{12}} \tau_{12} \\
 \gamma_{13} &= \frac{1}{G_{13}} \tau_{13} \\
 \gamma_{23} &= \frac{1}{G_{23}} \tau_{23}
 \end{aligned} \tag{2.9}$$

where the subscripts refer to the directions of anisotropy defined in the preceding paragraph. Solving for the stresses and writing the resulting equations in matrix form, one obtains

$$(\sigma') = [D'] (\epsilon') \tag{2.10}$$

where

$$(\sigma') = (\sigma_1 \ \sigma_2 \ \sigma_3 \ \sigma_{12} \ \sigma_{13} \ \sigma_{23})$$

$$(\epsilon') = (\epsilon_1 \ \epsilon_2 \ \epsilon_3 \ \gamma_{12} \ \gamma_{13} \ \gamma_{23})$$

and

$$[D']^{-1} = \begin{bmatrix}
 \frac{1}{E_1} - \frac{\nu_{12}}{E_2} - \frac{\nu_{13}}{E_3} & 0 & 0 & 0 & 0 & 0 \\
 \frac{1}{E_2} - \frac{\nu_{23}}{E_3} & 0 & 0 & 0 & 0 & 0 \\
 \frac{1}{E_3} & 0 & 0 & 0 & 0 & 0 \\
 & \frac{1}{G_{12}} & 0 & 0 & 0 & 0 \\
 \text{Symmetric} & & \frac{1}{G_{13}} & 0 & 0 & 0 \\
 & & & \frac{1}{G_{23}} & 0 & 0
 \end{bmatrix}$$

$$\begin{bmatrix}
 0 & \frac{1}{r_s} & 0 & \frac{\theta'}{r_s} & 0 & \frac{z'}{r_s} & 0 & \frac{\theta'z'}{r_s} & 0 & 0 & 0 & 0 & 0 & 0 \\
 \frac{1}{r_s} & \frac{\theta'}{r_s} & \frac{\theta'z'}{r_s} & \frac{r'\theta'}{r_s} & \frac{z'}{r_s} & \frac{r'z'}{r_s} & \frac{\theta'z'}{r_s} & \frac{r'\theta'z'}{r_s} & 0 & 0 & \frac{1}{r\theta_s} & \frac{r'}{r\theta_s} & 0 & 0 \\
 0 & 0 & 0 & 0 & 0 & 0 & 0 & 0 & 0 & 0 & 0 & 0 & 0 & 0 \\
 0 & 0 & \frac{1}{r\theta_s} & \frac{r'}{r\theta_s} & 0 & -\frac{1}{r} & \frac{1}{r_s} & -\frac{r'}{r_s} & -\frac{\theta'}{r_s} & \frac{\theta'}{r_s} & -\frac{r'\theta'}{r_s} & -\frac{z'}{r_s} & \frac{z'}{r_s} & -\frac{r'z'}{r_s} \\
 0 & 0 & 0 & 0 & \frac{1}{z_s} & \frac{r'}{z_s} & \frac{\theta'}{z_s} & \frac{r'\theta'}{z_s} & 0 & 0 & 0 & 0 & 0 & 0 \\
 0 & 0 & 0 & 0 & 0 & 0 & 0 & 0 & 0 & 0 & 0 & 0 & \frac{\theta'}{z_s} & \frac{r'\theta'}{z_s} \\
 \frac{z'}{r\theta_s} & \frac{r'z'}{r\theta_s} & 0 & 0 & 0 & 0 & 0 & 0 & 0 & 0 & 0 & 0 & 0 & 0 \\
 0 & 0 & 0 & 0 & 0 & 0 & 0 & 0 & 0 & \frac{1}{z_s} & \frac{r'}{z_s} & \frac{\theta'}{z_s} & \frac{r'\theta'}{z_s} & 0 \\
 -\frac{\theta'z'}{r_s} & \frac{\theta'z'}{r_s} & -\frac{r'\theta'z'}{r_s} & 0 & 0 & 0 & 0 & 0 & 0 & 0 & 0 & 0 & 0 & 0 \\
 0 & 0 & 0 & 0 & 0 & \frac{1}{r_s} & 0 & \frac{\theta'}{r_s} & 0 & \frac{z'}{r_s} & 0 & 0 & \frac{\theta'z'}{r_s} & 0 \\
 \frac{\theta'}{z_s} & \frac{r'\theta'}{z_s} & 0 & 0 & \frac{1}{r\theta_s} & \frac{r'}{r\theta_s} & 0 & \frac{z'}{r\theta_s} & 0 & 0 & \frac{z'}{r\theta_s} & 0 & \frac{r'z'}{r\theta_s} & \frac{r'z'}{r\theta_s}
 \end{bmatrix}$$

Table 2.2 The Matrix [q]

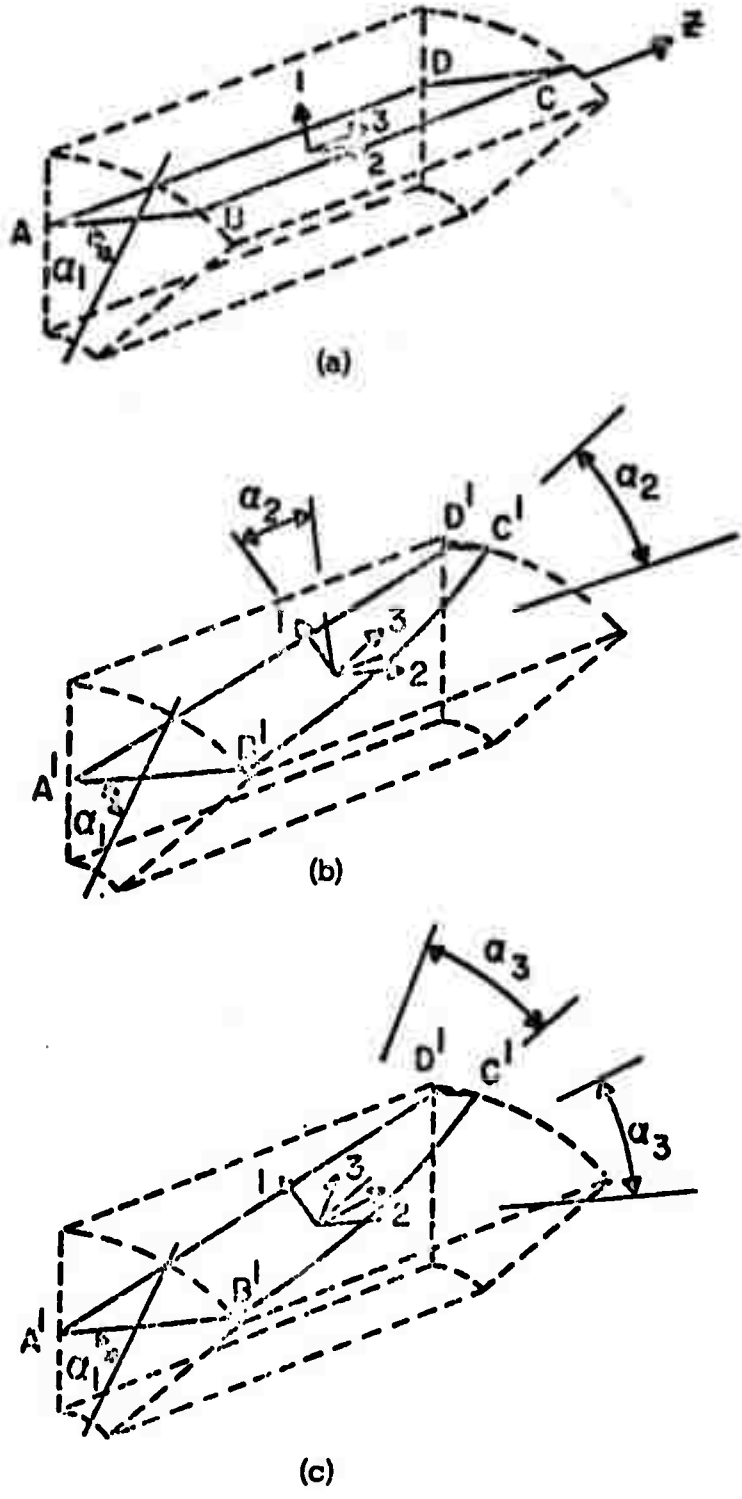


FIGURE 2.4 Step-by-step Orientation of Axes of Anisotropy

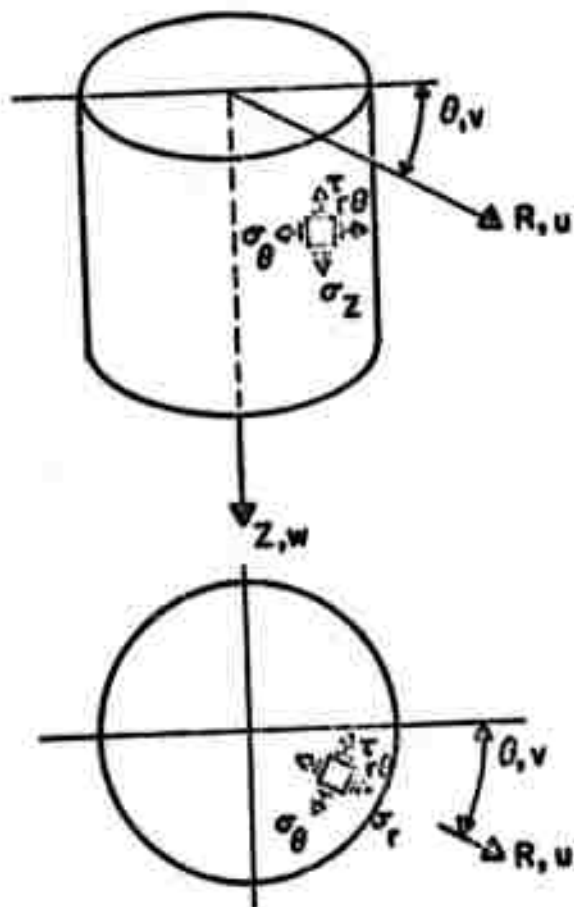


FIGURE 2. 5 Positive Direction of Stresses and Displacements

An equation connecting the stress vectors $\{\sigma\}$ and $\{\sigma'\}$ can be obtained from consideration of equilibrium of the tetrahedron shown in Fig. 2.6. Let, for example, the stresses σ_θ , $\tau_{r\theta}$ and $\tau_{\theta z}$ act on the inclined plane ABC. Furthermore, let (t_{21}, t_{22}, t_{23}) , (t_{11}, t_{12}, t_{13}) , and (t_{31}, t_{32}, t_{33}) be the direction cosines of these stresses relative to the axes 1, 2, 3. It can be shown that the components of stress acting on the plane ABC and parallel to the coordinate axes 1, 2, 3 are

$$\begin{aligned} R_1 &= \sigma_1 t_{21} + \tau_{12} t_{22} + \tau_{13} t_{23} \\ R_2 &= \tau_{12} t_{21} + \sigma_2 t_{22} + \tau_{23} t_{23} \\ R_3 &= \tau_{13} t_{21} + \tau_{23} t_{22} + \sigma_3 t_{23} \end{aligned} \quad (2.11)$$

The stress components σ_θ , $\tau_{r\theta}$ and $\tau_{\theta z}$ can then be calculated to be

$$\begin{aligned} \sigma_\theta &= R_1 t_{21} + R_2 t_{22} + R_3 t_{23} \\ \tau_{r\theta} &= R_1 t_{11} + R_2 t_{12} + R_3 t_{13} \\ \tau_{\theta z} &= R_1 t_{31} + R_2 t_{32} + R_3 t_{33} \end{aligned} \quad (2.12)$$

Similar expressions can be derived for σ_r , σ_z and τ_{rz} resulting in the general relationship

$$\{\sigma\} = [T] \{\sigma'\} \quad (2.13)$$

in which $[T]$ is a stress transformation matrix (Table 2.3). It can be shown that

$$[D] = [T] [D'] [T]^T \quad (2.14)$$

The table of direction cosines is given below:

Axes	1	2	3
R	t_{11}	t_{12}	t_{13}
θ	t_{21}	t_{22}	t_{23}
z	t_{31}	t_{32}	t_{33}

where

$$\begin{aligned}
t_{11} &= \cos \alpha_2 \sin(\alpha_1 - \theta_s \theta') \\
t_{21} &= -\cos \alpha_2 \cos(\alpha_1 - \theta_s \theta') \\
t_{31} &= -\sin \alpha_2 \\
t_{12} &= \cos \alpha_3 \cos(\alpha_1 - \theta_s \theta') + \sin \alpha_3 \sin \alpha_2 \sin(\alpha_1 - \theta_s \theta') \\
t_{22} &= \cos \alpha_3 \sin(\alpha_1 - \theta_s \theta') - \sin \alpha_3 \sin \alpha_2 \cos(\alpha_1 - \theta_s \theta') \\
t_{32} &= \sin \alpha_3 \cos \alpha_2 \\
t_{13} &= \cos \alpha_3 \sin \alpha_2 \sin(\alpha_1 - \theta_s \theta') - \sin \alpha_3 \cos(\alpha_1 - \theta_s \theta') \\
t_{23} &= -\cos \alpha_3 \sin \alpha_2 \cos(\alpha_1 - \theta_s \theta') - \sin \alpha_3 \sin(\alpha_1 - \theta_s \theta') \\
t_{33} &= \cos \alpha_3 \cos \alpha_2
\end{aligned} \tag{2.15}$$

The stiffness matrix of an element is

$$[k]^e = [c]^{-1T} \left(\int_{-1}^{+1} \int_{-1}^{+1} \int_{-1}^{+1} [q]^T [D][q] dV \right) [c]^{-1} \tag{2.16}$$

in which

$$dV = r r_s \theta_s z dr' d\theta' dz'$$

The integral portion of eq. (2.16) is evaluated by means of the Gaussian quadrature formula.

2.3 Formulation of Essential Matrices for Two-Dimensional Elements

The same relationships as in the preceding section, but with terms involving z and w and components of stress and strain in the direction of Z -axis eliminated, are used as bases to derive the matrices for two-dimensional elements. The displacement expression becomes simply

$$\begin{Bmatrix} u \\ v \end{Bmatrix} = \begin{bmatrix} 1 & r' & \theta' & r'\theta' & 0 & 0 & 0 & 0 \\ 0 & 0 & 0 & 0 & 1 & r' & \theta' & r'\theta' \end{bmatrix} \begin{Bmatrix} a_1 \\ a_2 \\ \vdots \\ a_8 \end{Bmatrix} \tag{2.17}$$

The matrix $[c]$ reduces to

t_{11}^2	t_{12}^2	t_{13}^2	$2t_{11}t_{12}$	$2t_{11}t_{13}$	$2t_{12}t_{13}$
t_{21}^2	t_{22}^2	t_{23}^2	$2t_{21}t_{22}$	$2t_{21}t_{23}$	$2t_{22}t_{23}$
t_{31}^2	t_{32}^2	t_{33}^2	$2t_{31}t_{32}$	$2t_{31}t_{33}$	$2t_{32}t_{33}$
$t_{11}t_{21}$	$t_{12}t_{22}$	$t_{13}t_{23}$	$t_{12}t_{21} + t_{11}t_{22}$	$t_{13}t_{21} + t_{11}t_{23}$	$t_{13}t_{22} + t_{12}t_{23}$
$t_{11}t_{31}$	$t_{12}t_{32}$	$t_{13}t_{33}$	$t_{12}t_{31} + t_{11}t_{32}$	$t_{13}t_{31} + t_{11}t_{33}$	$t_{13}t_{32} + t_{12}t_{33}$
$t_{21}t_{31}$	$t_{22}t_{32}$	$t_{23}t_{33}$	$t_{22}t_{31} + t_{21}t_{32}$	$t_{23}t_{31} + t_{21}t_{33}$	$t_{23}t_{32} + t_{22}t_{33}$

Table 2.3 The Transformation Matrix [T]

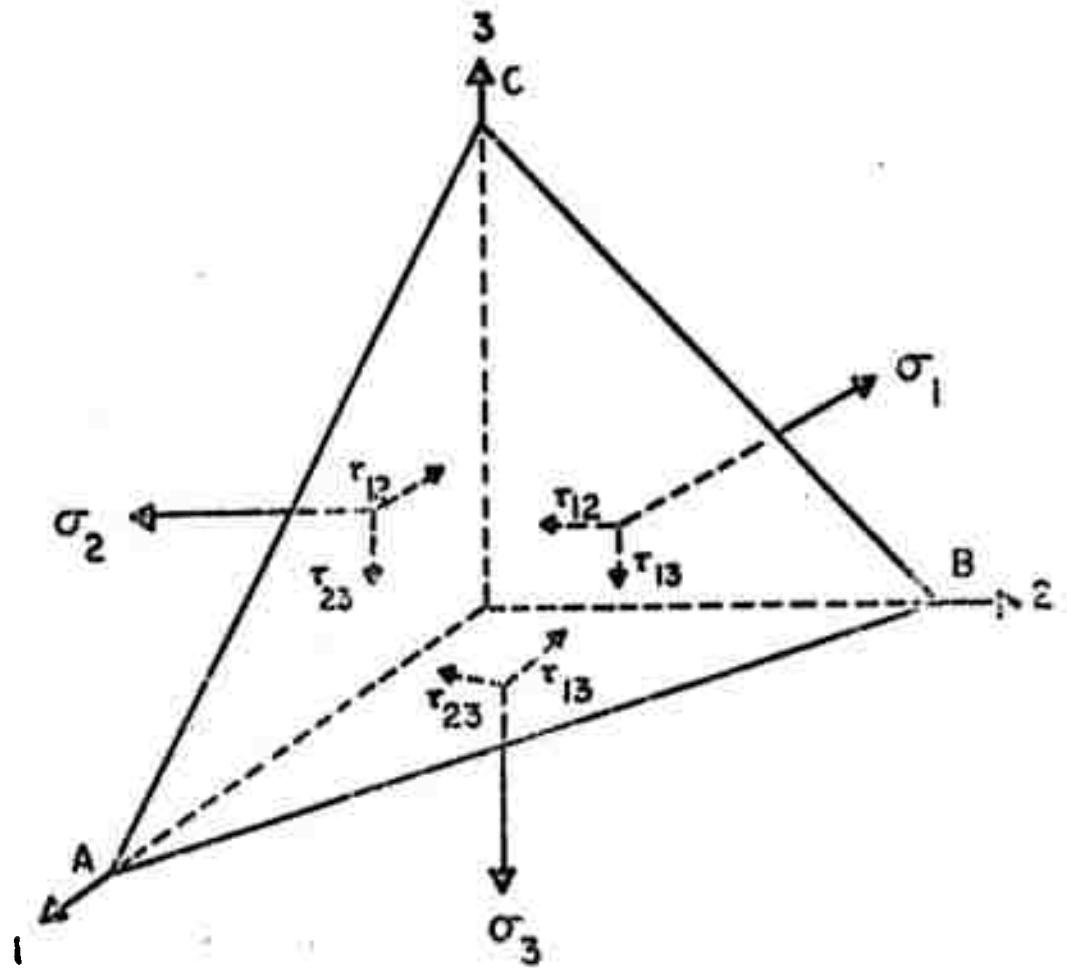
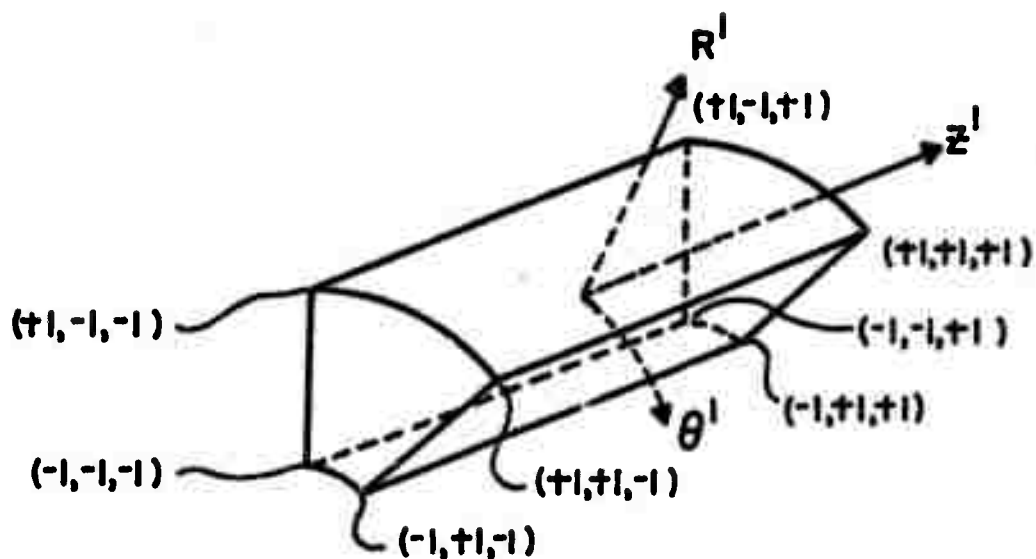
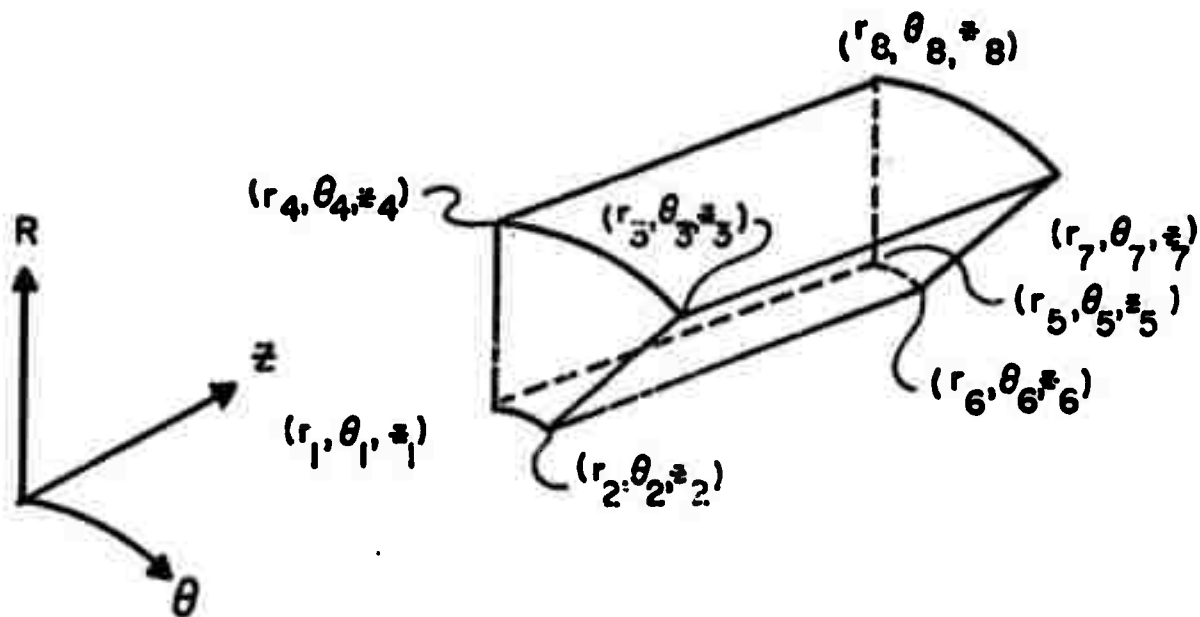


FIGURE 2.6 Stress Tetrahedron



(a) Local coordinates



(b) Global coordinates

FIGURE 2.7 Nodal Coordinates of Three-Dimensional Element

$$[c] = \begin{bmatrix} 1 & -1 & -1 & 1 & 0 & 0 & 0 & 0 \\ 0 & 0 & 0 & 0 & 1 & -1 & -1 & 1 \\ 1 & -1 & 1 & -1 & 0 & 0 & 0 & 0 \\ 0 & 0 & 0 & 0 & 1 & -1 & 1 & -1 \\ 1 & 1 & 1 & 1 & 0 & 0 & 0 & 0 \\ 0 & 0 & 0 & 0 & 1 & 1 & 1 & 1 \\ 1 & 1 & -1 & -1 & 0 & 0 & 0 & 0 \\ 0 & 0 & 0 & 0 & 1 & 1 & -1 & -1 \end{bmatrix} \quad (2.18)$$

and its inverse becomes

$$[c]^{-1} = \frac{1}{4} [c]^T \quad (2.19)$$

The formulas for components of strain are now

$$(\epsilon) = \begin{Bmatrix} \epsilon_r \\ \epsilon_\theta \\ \gamma_{r\theta} \end{Bmatrix} = \begin{Bmatrix} \frac{\partial u}{\partial r} \\ \frac{u}{r} + \frac{\partial v}{r\partial\theta} \\ \frac{\partial u}{r\partial\theta} + \frac{\partial v}{\partial r} - \frac{v}{r} \end{Bmatrix} \quad (2.20)$$

from which the matrix $[q]$ is obtained to be

$$[q] = \begin{bmatrix} 0 & \frac{1}{r_s} & 0 & \frac{\theta}{r_s} & 0 & 0 & 0 & 0 \\ \frac{1}{r} & \frac{r'}{r} & \frac{\theta'}{r} & \frac{r'\theta'}{r} & 0 & 0 & \frac{1}{r\theta_s} & \frac{r'}{r\theta_s} \\ 0 & 0 & \frac{1}{r\theta_s} & \frac{r'}{r\theta_s} & -\frac{1}{r} & \frac{1}{r_s} & -\frac{r'}{r} & -\frac{\theta'}{r_s} - \frac{r\theta'}{r} \end{bmatrix} \quad (2.21)$$

The elasticity matrix for plane stress is

$$[D] = \frac{E}{1-\nu^2} \begin{bmatrix} 1 & \nu & 0 \\ \nu & 1 & 0 \\ 0 & 0 & \frac{1-\nu}{2} \end{bmatrix} \quad (2.22)$$

Similarly, for anisotropic case

$$[D']^{-1} = \begin{bmatrix} \frac{1}{E_1} & -\frac{\nu}{E_2} & 0 \\ & \frac{1}{E_2} & 0 \\ \text{Sym.} & & \frac{1}{G_{12}} \end{bmatrix} \quad (2.23)$$

With $\{\sigma\}$ equal to $\{\sigma_r \sigma_\theta \tau_{r\theta}\}$, $\{\sigma'\}$ equal to $\{\sigma_1 \sigma_2 \tau_{12}\}$ and α_1 defined as in section 2.2, the stress transformation matrix is calculated to be

$$[T] = \begin{bmatrix} \sin^2 \alpha & \cos^2 \alpha & 2 \sin \alpha \cos \alpha \\ \cos^2 \alpha & \sin^2 \alpha & -2 \sin \alpha \cos \alpha \\ -\sin \alpha \cos \alpha & \sin \alpha \cos \alpha & \sin^2 \alpha - \cos^2 \alpha \end{bmatrix} \quad (2.24)$$

in which $\alpha = \alpha_1 - \theta_s \theta'$.

In the element stiffness expression [eq. (2.22)],

$$dV = r t r_s \theta_s dr' d\theta \quad (2.25)$$

in which t is the thickness of the disc.

It should be noted that all the matrices, except $[D]$, formed in this section could also have been obtained directly from the three-dimensional matrices of the preceding section by simply deleting appropriate rows and columns of the latter and setting values of certain parameters to zero. In particular, to obtain $[c]$, rows 3, 6, 9 and 12 to 24 and columns 5 to 8 and 13 to 24 of Table 2.1 are deleted; to obtain $[q]$ rows 3, 5 and 6 and columns 5 to 8 and 13 to 24 of Table 2.2 are deleted; to obtain $[T]$ rows and columns 3, 5 and 6 of Table 2.3 are deleted and α_2 and α_3 are set to zero. Thus, by adding a few IF statements to and generalizing some indices of a three-dimensional computer program, the program can be made to work for two-dimensional cases as well.

2.4 Failure Criteria

The analysis described in this chapter will be based on any one or combination of the following failure criteria:

1. Maximum principal stress theory--

Under this criterion, an element will be considered failed if one of the principal stresses equals or exceeds the strength (elastic limit or yield point) of the material making up the element. If tensile failure occurs, the modulus of elasticity across the crack is reduced to zero and the stiffness of the element is revised accordingly. The element can therefore no longer resist tensile stress (no stress reversal is anticipated) normal to the crack but can still take tension or compression in the other directions.

If failure occurs in compression (crushing), an approximation is made. To account for the fact that rock exhibits ductility when subjected to high confining pressure, only a portion of the stiffness of the failed element will be removed. A more realistic approach would be to undertake inelastic analysis to obtain the actual stiffness of the failed element. This approach, however, presupposes the availability of a stress-strain curve which might not be feasible in most rocks. Indeed, such curve can only be obtained through a triaxial test and its shape will vary widely depending on, among other factors, the rock type, shape of specimen, and intensity of confining pressure. Stress-strain curves of few rocks are available (1) but only at certain confining pressure intensities.

2. Maximum shearing stress theory--

This criterion states that failure occurs when the maximum shearing stress in a material equals or exceeds the critical shearing stress. The Coulomb-Navier (1) version will be used. This states that shearing failure will occur when

$$\sigma_1(-\mu + \sqrt{\mu^2 + 1}) - \sigma_3(\mu + \sqrt{\mu^2 + 1}) \geq 2\tau_{cr} \quad (2.26)$$

in which τ_{cr} is the critical shearing stress found to be between 2% and 15% of uniaxial compressive strength; μ is the coefficient of internal friction; and σ_1 and σ_3 are the major and minor principal stresses. The above expression takes into account frictional resistance to sliding along the failure plane.

It should be noted that if $\mu = 0$, that is, there is no frictional resistance, the above inequality reduces to

$$\sigma_1 - \sigma_3 \geq 2 \tau_{cr} \quad (2.27)$$

in which the left side is simply the expression for twice the maximum shearing stress at a point.

Again, post-failure behavior of elements will be approximated.

3. Maximum principal strain theory--

This could be a better alternative to the first criterion in the sense that here effects of the other principal stresses acting normal to the direction being investigated are considered. To illustrate this point, consider Fig. 2.8. Let σ_e be the critical stress and ϵ_e the corresponding strain. In the first figure, both the first and the present criteria will predict the same failure stress, namely, $\sigma_1 = \sigma_e$. In the second figure, the first criterion will predict the failure condition $\sigma_1 = \sigma_e$, but the present criterion will predict a value greater than σ_e since failure occurs when $(\sigma_1 - \nu\sigma_2) \geq \epsilon_e E$. Similarly, a value less than σ_e will be predicted if σ_2 is in tension.

Failed elements will be treated the same way as in the first criterion.

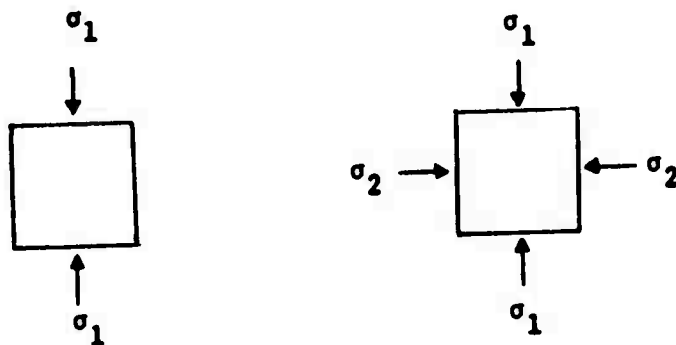


Figure 2.8

2.5 Concluding Remarks

Derived in this chapter are the different matrices needed in the development of the finite element program proposed in this report. Discussion of such other integral parts of the program as (a) building up of the global stiffness matrix, (b) determination of nodal displacements and stresses, and (c) calculation of principal stresses is omitted because they are discussed in detail elsewhere (2, 3, 5, 6).

An equation solver proposed by Jensen and Parks (6) will be used in the program. The solver contains an optimal nodal renumbering scheme to conserve sparseness of the stiffness matrix. Only nonzero terms of the matrix are stored and processed.

REFERENCES

1. Farmer, I. W., Engineering Properties of Rocks, E & FN Spon Ltd., London, 1968.
2. Timoshenko, S. and J. N. Goodier, Theory of Elasticity, McGraw-Hill Book Company, Inc., New York, 1951.
3. Zienkiewicz, O. C. and Y. K. Cheung, The Finite Element Method in Structural and Continuum Mechanics, McGraw-Hill Book Co., London, 1967.
4. Zienkiewicz, O. C., S. Valliappan, and I. P. King, "Stress Analysis of Rock as a 'No Tension' Material," Geotechnique, Vol. 18, March 1968, pp. 56-66.
5. Basas, J. E. "Static Analysis of Stiffened Shells by the Finite Element Method," Ph. D. Dissertation, Department of Civil Engineering, University of Wisconsin, Madison, Wisconsin, 1971.
6. Jensen, H. G. and G. A. Parks, "Efficient Solutions for Linear Matrix Equations," Journal of the Structural Division, Proc. ASCE, Vol. 96, No. ST1, Jan. 1970, pp. 49-64.
7. Seely, F. B. and J. O. Smith, Advanced Mechanics of Materials, John Wiley & Sons, Inc., New York, 1932.

CHAPTER 3

TWO-DIMENSIONAL PROGRAM

3.1 Introduction

The program described herein was developed as an alternative to the two-dimensional program submitted as part of the first annual progress report (1). It contains the following features not found in the earlier program:

1. Element and node information are generated automatically thus avoiding the preparation of voluminous deck of input cards.
2. Element sizes may vary, allowing for finer mesh in regions where stresses are large and coarser mesh elsewhere, for a more efficient solution.
3. More than one element may fail during each loading cycle.

No change is made in the failure criteria.

The element used in the present program is shown in Fig. 2.1 and described in section 2.3. The element belongs to the so-called "isoparametric" group.

3.2 Description of Program

The flow of the program is illustrated in Fig. 3.2. The total program is made up of the main program and four subroutines (complete listing is shown in Appendix A). Each performs the following tasks:

Main Program

- generates element and node numbers in the sequence shown in Fig. 3.1;
- generates the nodal coordinates, given the radial coordinates of the rings and the circumferential coordinates of the radial lines;
- forms the global stiffness matrix in blocks;
- calculates the stresses and load factors (ratio of allowable stress to principal stress) of each element;

- calculates critical loads, displacements and strains; and
- removes 90% of stiffness matrix of failed elements from global stiffness matrix.

Subroutine DISPL

- evaluates the unknown nodal displacements by the Gaussian elimination method and back-substitution.

Subroutine MATB

- forms the matrix $[q]$ and the matrix product $[D][q]$.

Subroutine INTEG

- forms the stiffness matrix of the elements, employing Gaussian quadrature formulas in place of actual analytical integration.

Subroutine UNIFRM

- generates elastic properties of elements of nonhomogeneous disc by means of the random number routine RANUN (2).

RANUN generates arbitrary random numbers assuming statistically uniform distribution. The first generative number of RANUN can be set to any number N by a call to RANUNS(N). Both RANUN and RANUNS are Madison Academic Computing Center (MACC) library routines.

It should be noted that in numbering the nodes, the center point of the disc is multinumbered (see Fig. 3. 1). This is done because each element has to have four nodes.

The well-known banded matrix technique in solving simultaneous linear equations is employed in the program.

3. 3 Test Problems

Several problems were run to test the correctness of the program. The results of three are presented here.

A. Test Problem No. 1

A disc, 20 inches in diameter and 1 inch thick, is analyzed. It is required to determine the stress distribution along the line of the load.

The disc is assumed homogeneous and isotropic.

Because of symmetry, only a quarter of the disc is considered in the analysis. The quarter disc is divided into 25 rings and 18 equal slices for a total of 408 elements and 450 nodes. The results are shown in Fig. 3.3.

B. Test Problem No. 2 (Homogeneous Case)

A homogeneous disc, 3 inches in diameter, 1 inch thick, and possessing the following elastic properties

Modulus of elasticity :	5.7×10^6 psi
Poisson's ratio :	0.25
Allowable compression:	27,000 psi
Allowable tension :	5% of allowable compression

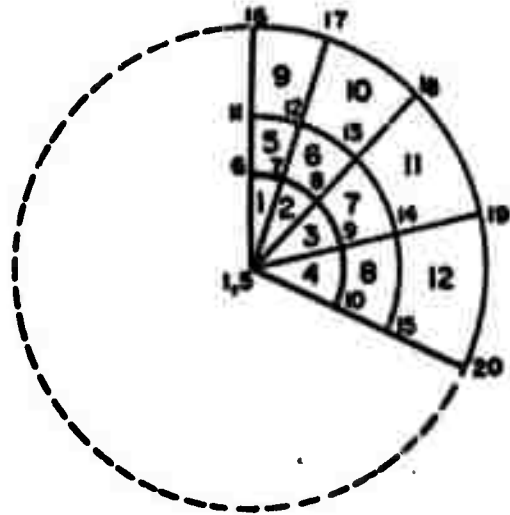
is analyzed. The disc is divided into the mesh shown in Fig. 3.4. A listing of the required input data is printed on page 50. Some of the results of the analysis are indicated in the following pages.

C. Test Problem No.3 (Nonhomogeneous Case)

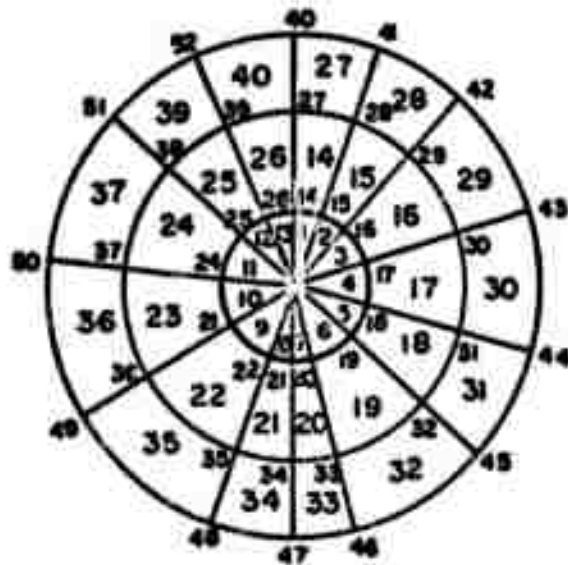
A nonhomogeneous disc, 3 inches in diameter and 1 inch thick, is analyzed. The elastic properties of the elements vary as follows:

Modulus of elasticity :	5.5×10^6 to 6.5×10^6 psi
Poisson's ratio :	0.23 to 0.27
Allowable compression:	22,000 to 32,000 psi
(allowable tension = 5% of allowable compression)	

Double symmetry is assumed to avoid having to analyze the entire disc which would require considerably higher computer expense. The disc is divided into the same mesh shown in Fig. 3.4. Several runs were made. During each run, a different starting point for the random number generator was specified. The necessary input is listed on page 51. Results of the analysis are indicated in the following pages.

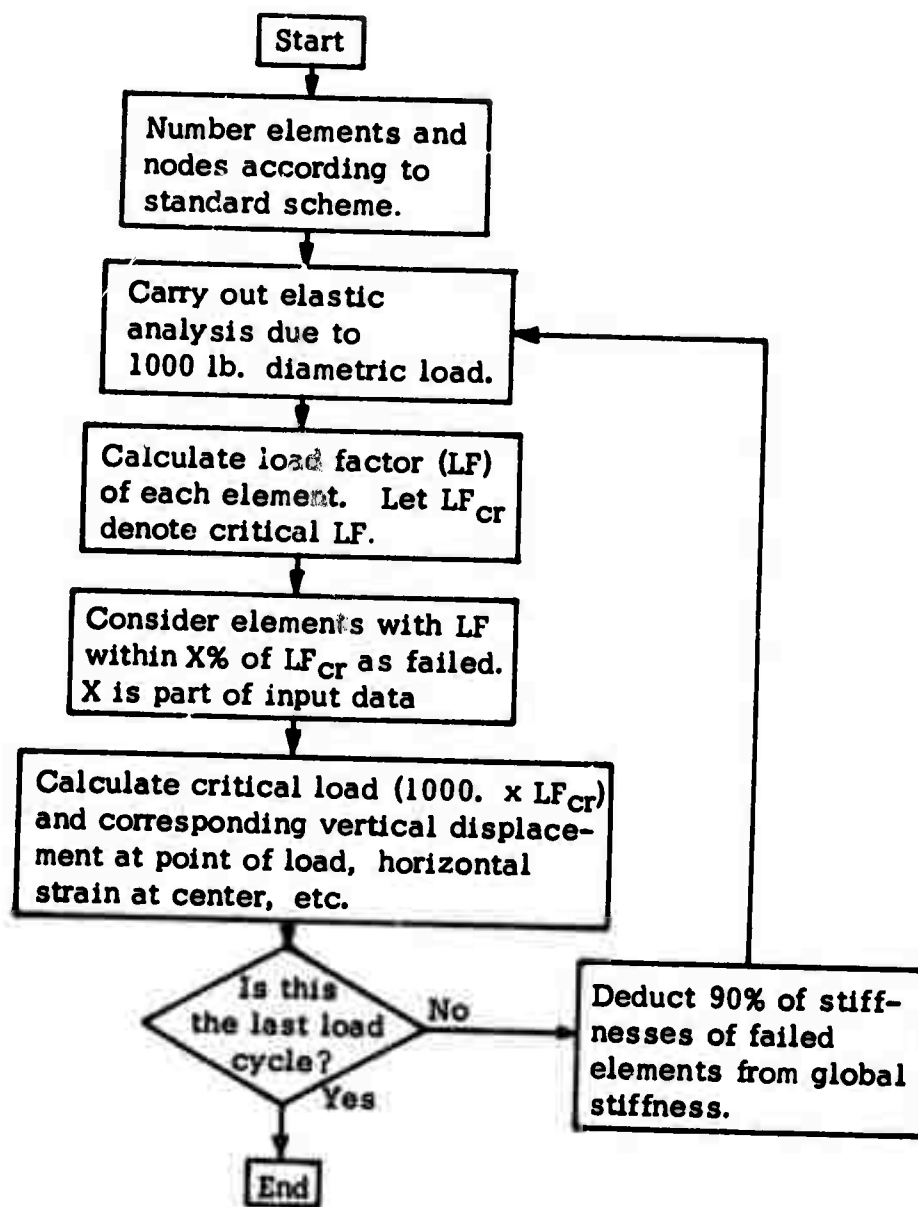


(a) Partial Disc



(b) Full Disc

FIGURE 3.1 Standard Scheme for Numbering Nodes and Elements of Two-Dimensional Disc



Note: Load factor is the ratio of allowable stress to principal stress.

FIGURE 3.2 FLOW CHART OF TWO-DIMENSIONAL PROGRAM.

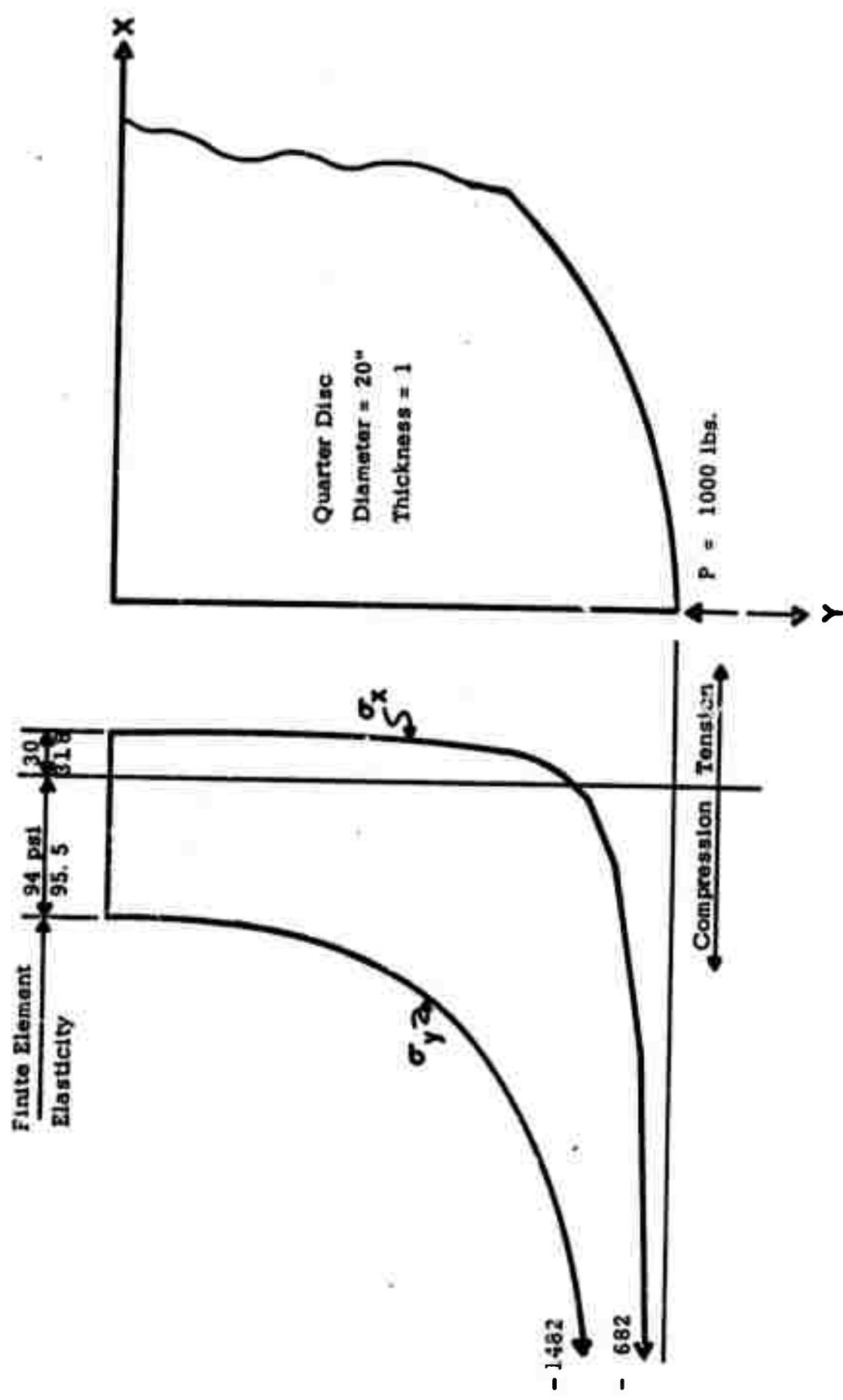
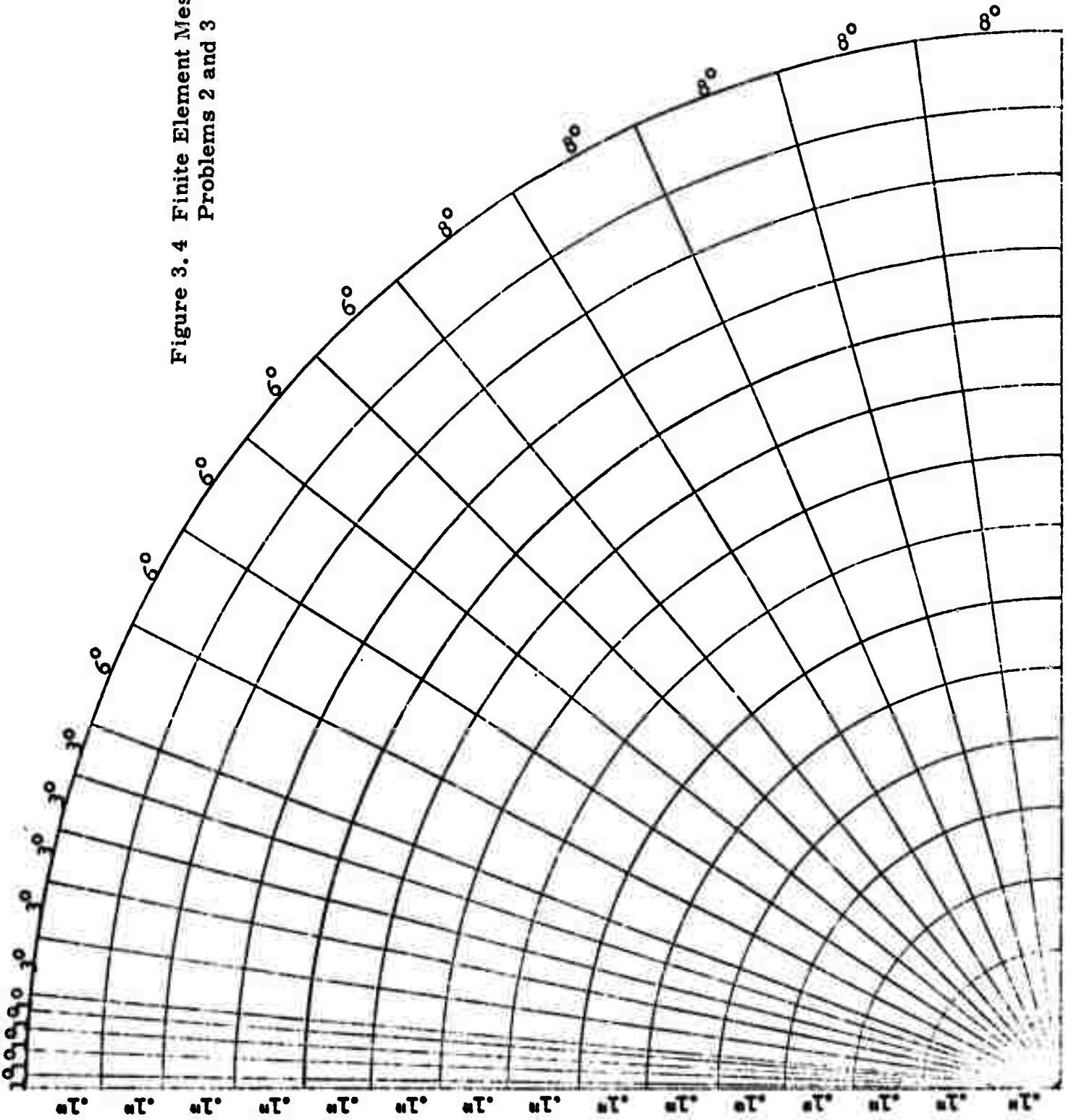


FIGURE 3.3 Stress Distribution Along Line of Diametral Load (Test Problem No. 1)

Figure 3.4 Finite Element Mesh for Problems 2 and 3



INPUT DATA FOR TEST PROBLEM NO. 2 (HOMOGENEOUS CASE)

Column													Card No.														
1	5	6	10	11	15	16	20	21	25	26	30	31	35	36	40	41	45	46	50	51	55	56	60	61	65	66	
																											1
																											2
																											3
																											4
																											5
																											6
																											7
																											8
																											9
																											10
																											11
																											12
																											13

Reproduced from
 Best available copy

INPUT DATA FOR TEST PROBLEM NO. 3 (NONHOMOGENEOUS CASE)

		Column														Card No.										
1	56	10	11	15	16	20	21	25	26	30	31	35	36	40	41	45	46	50	51	55	56	60	61	65	66	1
	1	214	21	47																						2
	550000.	650000.	220000.																							3.
	1	0																								3
	300	336	51	1	20	0	16	5	20																	4
	3962185281																									5
	0.	.1	.2																							6
	.9	1.	1.1	1.2																						7
	0.	1.	2.	3.																						8
	17.	20.	26.	32.																						9
	74.	82.	90.																							10
	1316	500.																								11
	1		20	1																						12
	22200.		14	21																						13
	42200.		14	21																						14

NOTE: In this set of data, starting point of random number generator is N = 3962185381 (Card No. 5)

3.4 Discussion of Results

The results from Test Problem No. 1 clearly demonstrate the theoretical correctness of the finite element solution formulated in this report. As can be seen from Fig. 3.3, the elasticity and finite element solutions differ by only 6% for σ_x and 2% for σ_y at the center of the disc. By solving the same problem several times progressively decreasing element size each time, the finite element solution was also found to be convergent.

The discs analyzed in Test Problems No. 2 and No. 3 are models for the Valdres limestones studied extensively in the experimental phase of this research (Chapter 1). The elastic properties assigned to the nonhomogeneous disc are actual range of values obtained from experiment, while those assigned to the homogeneous disc are the mean of these values. The failure pattern predicted by the finite element solution (Figs. 3.5 and 3.6) agrees favorably with the actual failure patterns of Brazilian tests. The critical load, however, appears to be underestimated--5730 lbs. and 4400 lbs. for homogeneous and nonhomogeneous cases compared to the 6940 lbs. average obtained from the experiment. This seems to indicate that either the 90% factor used to deduct the stiffness matrix of failed elements is too high or the failure mechanism assumed in the program is not altogether realistic or both.

The load-displacement curves appear to follow the same general shape regardless of material characteristics or starting point of random number generator (see Figs. 3.7 and 3.8). These curves compare favorable with those obtained from the experiment at the early stages of loading.

3.5 Conclusions

Based on the several computer runs made, the following conclusions are drawn:

1. Even in its oversimplified form, the finite element solution is capable of predicting the actual failure pattern of Brazilian tests.
2. With a few improvements in the failure criteria, there is a strong

possibility that the critical load and the load-displacement curve can be accurately predicted as well.

3. In nonhomogeneous cases, the shape of the load-displacement curve is not affected significantly by the choice of the starting point of the random number generator.

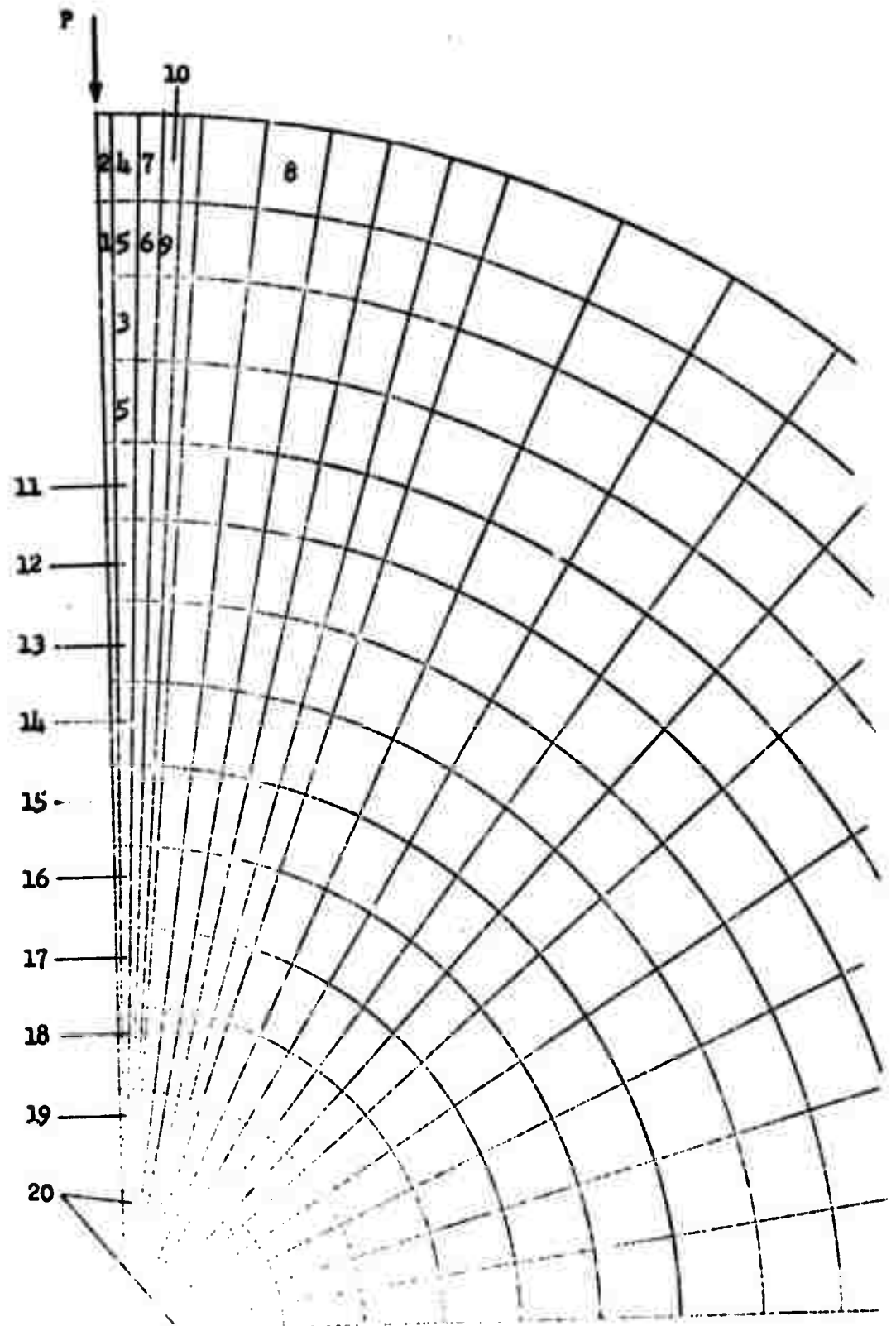


Figure 3.5 Progression of Failure in Test Problem No. 2

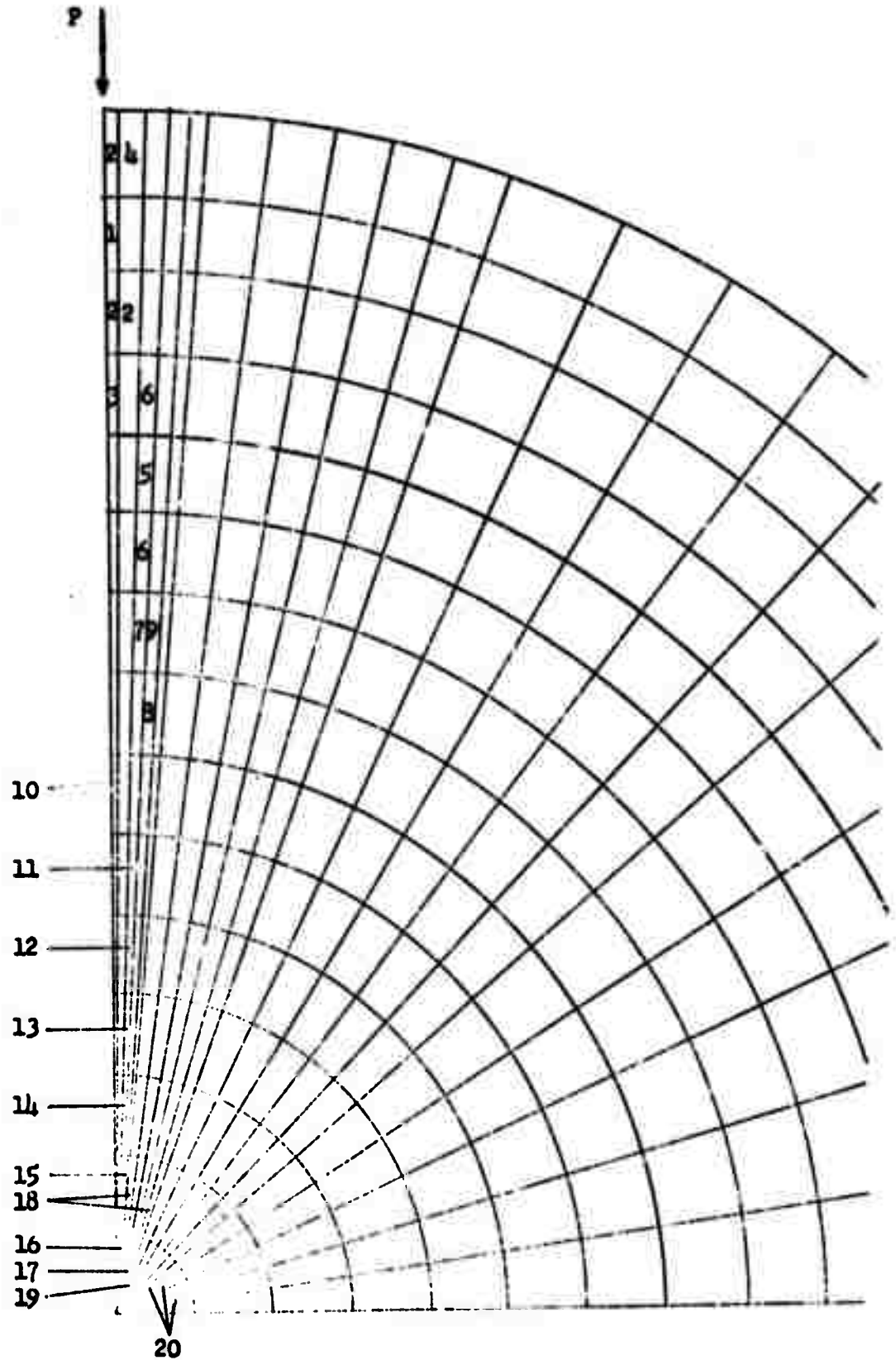


Figure 3.6 Progression of Failure in Test Problem No. 3

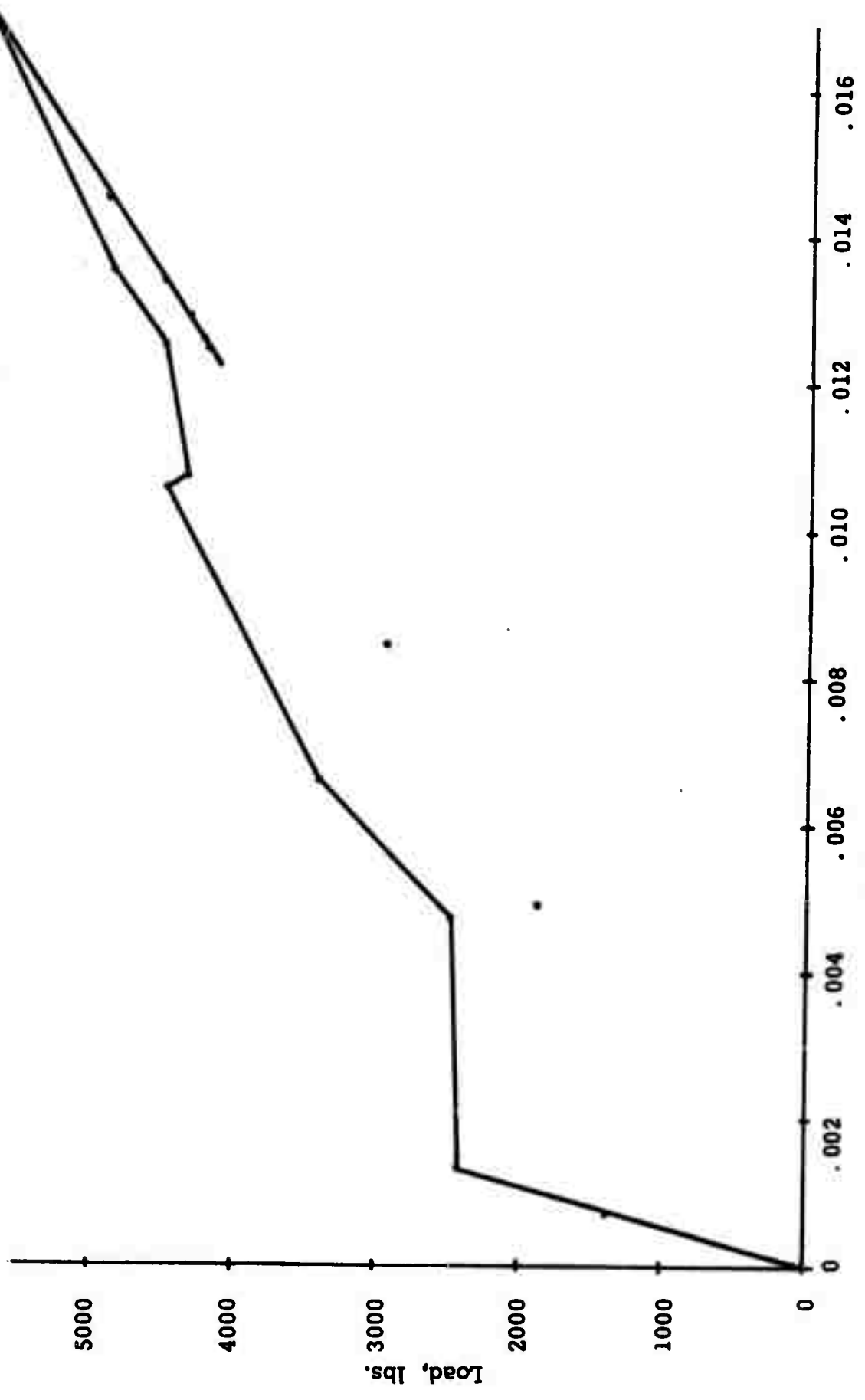


FIGURE 3.7 Load-Displacement Curve (Homogeneous Case)

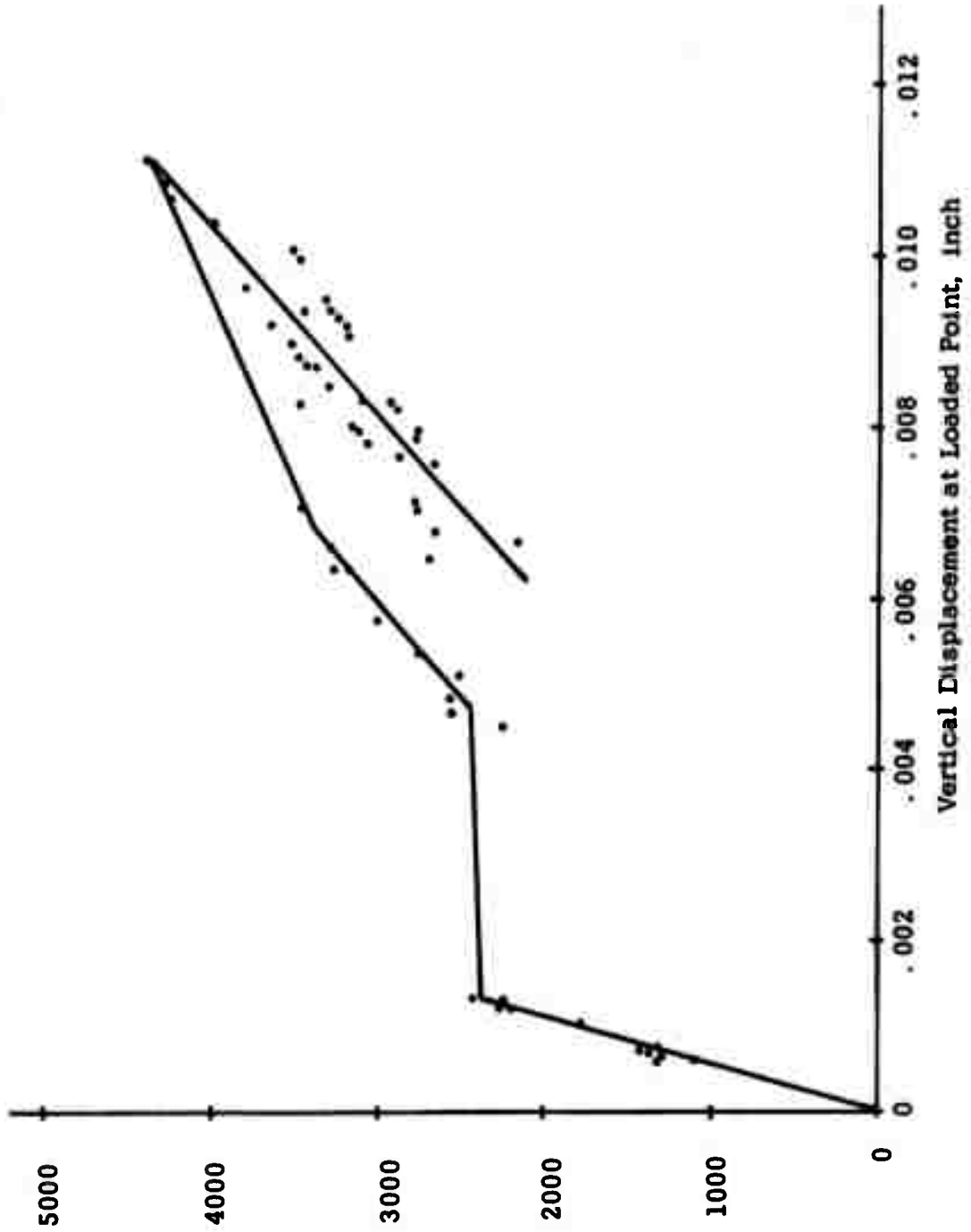


FIGURE 3.8 Load-Displacement Curve (Nonhomogeneous Case)

REFERENCES

1. Aspects of Mechanical Behavior of Rock Under Static and Cyclic Loading (Part A--Mechanical Behavior of Rock under Static Loading), Annual Technical Progress Report, Engineering Experiment Station, University of Wisconsin - Madison, March 1972.
2. Madison Academic Computing Center, Random Number Routines, Mathematical Routines Series, October 1969.
3. Basas, J. E., Static Analysis of Stiffened Shells by the Finite Element Method, Ph. D. Dissertation, Department of Civil Engineering, University of Wisconsin, Madison, Wisconsin, 1971.

APPENDIX A

TWO-DIMENSIONAL PROGRAM LISTING

The computer program presented here is written in Fortran V language specifically for the Univac 1108 computer at the University of Wisconsin - Madison. The program is capable of handling all sorts of static two-dimensional loadings, not just the diametric loading of the Brazilian test. Zero or nonzero displacements may be assigned to any node making possible solutions involving portions of the disc only.

The program requires usage of three auxiliary storage tapes or drums designated by the numbers 10, 11 and 12.

The listing is complete except for the random number routines RANUN(R) and RANUNS(N). These subprograms are provided by the Madison Academic Computing Center (MACC).

A description of the input and output parameters required in the program is given below.

Input Notations:

1. (a) NCHO - Printout code; 0 if only stresses at failed elements are to be printed out; nonzero if stresses at all elements are to be printed out.
- (b) NWCL - Node at which radial displacement is to be computed.
- (c) NST1, NST2 - Nodes between which strain is to be computed.
2. (a) EM1, EM2 - Range of values of elastic moduli.
- (b) CS1, CS2 - Range of values of allowable compressive stresses.
- (c) PR1, PR2 - Range of values of Poisson's ratios.
- (d) CTRAT - Ratio of allowable tension to allowable compression.
- (e) T - Thickness of disc.
- (f) TRN - Maximum percentage variation from largest load factor for element to be considered failed; 0 if only one element is allowed to fail each time.

- (g) DIA - Diameter of disc.
- 3. (a) IRN - Total number of elements in vicinity of applied loads.
- (b) NIK(I) - Number of Ith element in vicinity of applied loads; specified if run is to be terminated upon failure of element; 0 if run is to continue.
- 4. (a) NELEM - Total number of elements.
- (b) NTNN - Total number of nodes.
- (c) NNSD - Total number of nodes with prescribed displacements.
- (d) NNCL - Total number of nodes at which concentrated loads are applied.
- (e) NE - Total number of slices portion of disc involved in analysis is divided into.
- (f) NS - Total number of equal slices whole disc is divided into; 0 if disc is not divided into equal slices and only a portion of whole disc is involved in analysis; any negative number if disc is not divided into equal slices and whole disc is involved in analysis.
- (g) NC - Total number of rings plus one disc is divided into.
- (h) NER - Least total number of similar consecutively numbered elements; 1 in nonhomogeneous and anisotropic problems. This parameter allows the generation of stiffness matrix of similar elements only once.
- (i) NCOD - Total number of load cycles.
- 5. N - First generative number of random number routine. (Note that this information is supplied only in nonhomogeneous problems.)
- 6. RADN(I) - Radial coordinates of rings starting with 0.
- 7. TTAN(I) - Circumferential coordinates in degrees of radial lines dividing disc into slices. (Note that this information is supplied only when disc is divided into unequal slices.)

8. (a) MR - 1 for 1st card; 2 for 2nd card; 3 for 3rd card, etc.
- (b) NODC(MR) - Number of MRth node with externally applied concentrated load.
- (c) CLOAD(MR, I) - Magnitude of concentrated load. (I = 1 in radial direction; I = 2 in circumferential direction.)
9. (a) NODB(IX) - Number of IXth node with prescribed displacement.
- (b) DISP(IX, I) - Value of prescribed displacement; 200. if displacement is not prescribed. (I = 1 in radial direction; I = 2 in circumferential direction.)
- (c) JJ - Total number of nodes which exactly have the same prescribed displacements as NODB and which form an arithmetic progression with NODB; 0 if none such nodes.
- (d) II - Interval of arithmetic progression.

Output Notations:

- RADIAL** - Direct stress in radial direction.
- CIRCUM** - Direct stress in circumferential direction.
- SHEAR** - Shearing stress.
- PRNCP1, PRNCP2** - Principal stresses.
- MAXSHR** - Maximum shearing stress.
- LD FAC** - Load factor (ratio of allowable stress to actual stress).

All other output notations are self-explanatory.

```

1. C ANALYSIS OF CIRCULAR DISC
2. COMMON/JACKP/C(4,4),P(3,2),FL(3),SL(8,2),RR(3,2)
3. COMMON/COLOC/NTNN,NEM,NEN,NLB,F(200),S(200,100)
4. COMMON/ROPAR/PP,F,T,TCR,CCR
5. COMMON/TNATK/TTA(50),RAD(50),NOD(50,4)
6. COMMON/KRING/X1,X2,Y1,Y2,X(3),Y(3),Z(3),M,N
7. DIMENSION NODC(10),CLOAD(10,2),NODF(150),
8. IOTSP(150,2),RADN(100),TTAN(100),GA(5),GR(5),
9. ZOL(5),FOD(50,2),Z2(50,6),FLDF(50),
10. INFL(50),KEF(50),NJK(20)
11. DATA (GA(1),I=1,5)/-1.,-1.,1.,1.,0./
12. DATA (GA(2),I=1,5)/-1.,1.,1.,-1.,0./
13. DATA (C(1,T),T=1,4)/.25.,.25.,.25.,.25./
14. DATA (C(2,T),T=1,4)/-.25.,-.25.,.25.,.25./
15. DATA (C(3,T),T=1,4)/-.25.,.25.,.25.,-.25./
16. DATA (C(4,T),T=1,4)/.25.,-.25.,.25.,-.25./
17. DO 20 I=1,3
18. DO 30 J=1,8
19.
20. B(I,J)=0.
21. READ 1005,NCHO,NMCL,NST1,NST2
22. 1005 FORMAT (4I5)
23. READ 1000,FM1,FM2,CS1,CS2,PR1,PR2,CTRAT,T,TPN,OIA
24. 1000 FORMAT (4F10,3,EF5,1)
25. PRINT 1006,FM1,FM2
26. 1006 FORMAT (18H)ELASTIC MODULUS = ,1FE12.8,4H TO ,1FF12.F)
27. PRINT 1007,PR1,PR2
28. 1007 FORMAT (18H)POISSONS RATIO = ,F10.5,4H TO ,F11.5)
29. PRINT 1008,CS1,CS2
30. 1008 FORMAT (18H)CRITICAL COMPRESSIVE STRESS = ,
31. 12FE10.3,4H TO ,2FE10.3)
32. PRINT 1009,CTRAT
33. 1009 FORMAT (18H)CRITICAL TENSION/COMPRESSION RATIO = ,F5.2)
34. PRINT 1010,T
35. 1010 FORMAT (20H)THICKNESS OF DISC = ,F5.2)
36. PRINT 1011,OIA
37. 1011 FORMAT (18H)DIAMETER OF DISC = ,F5.2)
38. READ 1001,IBN,INX(I),I=1,IRN)
39. READ 1001,NFLEN,NTNN,NNSD,MNCL,NF,NS,NC,NFR,NCDD
40. 1001 FORMAT (21F)
41. NC=NC-1
42. PRINT 1012,NFLEN
43. 1012 FORMAT (20H)TOTAL NUMBER OF ELEMENTS = ,I3)
44. PRINT 1013,NTNN
45. 1013 FORMAT (20H)TOTAL NUMBER OF NODES = ,I3)
46. PRINT 1014,NF,NC)
47. 1014 FORMAT (41H)DISC IS DIVIDED INTO ,
48. I7,12H SLICES AND ,I7,1H RINGS)
49. TO (ABS(FM1-FM2)-.00001)113,113,131
50. 1131 READ 1100,N
51. 1132 FORMAT (1I4)
52. CALL RANUN(3)
53. DO 100 T=1,NFLEN
54. CALL UNIFRM (FM1,FM2,FNS)
55. CALL UNIFRM (PR1,PR2,PRS)
56. CALL UNIFRM (CS1,CS2,CSS)

```



```

55.      POUT,1)=FMS
56.      POUT,2)=FR5
57.      100 POUT,3)=CSS
58.      PRINT 1102,P0(2,1),P0(3,1)
59.      1100 FORMAT (1FF12.F,1FF12.F)
60.      GO TO 107
61.
62.      137 DO 101 I=1,NFLEM
63.          POUT,1)=FM1
64.          POUT,2)=FM1
65.      101 POUT,3)=CSI
66.      102 PRINT 6997
67.      6997 FORMAT (8H0FLEMEN,6X,12HCORNER NODES,3X,8H FLEMEN,
68.          10X,12HCORNER NODES)
69.      7010 FORMAT (5T6)
70.          TF (NE-NS)91,91,137
71.      137 TF (NS)91,91,30
72.          DO 200 I=1,NFLEM
73.              NOD(I,1)=I*(I-1)/NF
74.              NOD(I,2)=NOD(I,1)+1
75.              NOD(I,3)=NOD(I,2)+1+NE
76.              NOD(I,4)=NOD(I,3)-1
77.      200 CONTINUE
78.          NPM=(NE+3)*3
79.          GO TO 158
80.
81.      51 DO 199 I=1,NFLEM
82.          NOD(I,1)=I
83.          NOD(I,2)=I+1
84.          NOD(I,3)=NOD(I,2)+NE
85.          NOD(I,4)=NOD(I,3)-1
86.      199 CONTINUE
87.          NPM=NE*4
88.          DO 198 I=NE,NFLEM,NE
89.              NOD(I,2)=NOD(I,2)-NE
90.              NOD(I,3)=NOD(I,3)-NE
91.      198 CONTINUE
92.      170 NG=NFLM/2
93.          NC1=(NFLEM+1)/2
94.          DO 33 I=1,NG
95.              K=I+NG1
96.              PRINT 36,I,(NOD(I,J),J=1,4),K,(NOD(K,J),J=1,4)
97.
98.          26 CONTINUE
99.          76 FORMAT (5I6,4X,5T6)
100.         IF (NG-NG1)59,197,75
101.         75 PRINT 7010,NG1,(NOD(NG1),J),J=1,4)
102.         C..... GENERATE NODAL COORDINATES.....
103.         197 READ 1002,(RADN(I),I=1,NC)
104.         1002 FORMAT (9F8,3)
105.         TF (NE-NS)134,193,137
106.         137 IF (NS)193,194,194
107.         193 NE=NE-1
108.         194 DO 196 I=1,NTNK
109.             NOUN=1+(I-1)/(NE+1)
110.             RAD(I)=RADN(NOUN)
111.         196 CONTINUE
112.             NE=NE+1
113.             TF (NS)201,201,202
114.         201 READ 1002,(TTAN(I),I=1,NE)

```

```

113.      GO TO 200
114.      200  MNS=NS
115.          DUM=7E11./HNS
116.          DO 203 I=1,NF
117.              AI=I
118.              203  TTANCTI=(AI-1.)*DUM
119.              204  DO 195 I=1,NE
120.                  TT=I*NF*(NC-1)
121.                  TDUM=TTANCTI*.0174533
122.                  DO 192 J=1,NI*NF
123.                      192  TTACJI=TDUM
124.                      195  CONTINUE
125.                  PRINT 1015, (RADN(TI),I=1,NC)
126.          1015  FORMAT (13H/RADIAL COORDINATES/(GX,BF11.2))
127.                  PRINT 1016, (TTAN(TI),I=1,NF)
128.          1016  FORMAT (13H/CIRCUMFERENTIAL COORDINATES (DEGREES)
129.                  /14EX,BF10.2))
130.      C*****INPUT MAGNITUDES OF CONCENTRATED LOADS IF ANY*****
131.          IF (NNCL)2001,2001,2000
132.          2000  READ 1003,MR,NDDC(MR), (CLOAD(MR,I),I=1,2)
133.          1003  FORMAT (I2,I3,2F10.1)
134.          IF (MR>NNCL)2000,2001,2001
135.      C*****INPUT VALUES OF SPECIFIED DISPLACEMENTS*****
136.          2001  IX=0
137.          2004  IX=IX+1
138.          READ 1004,NDDC(IX), (DISP(IX,I),I=1,2),JJ,IT
139.          1004  FORMAT (I5,2F5.1,I3,I3)
140.          NDDM=IX
141.          IF (IX>NNSD)253,2002,2002
142.          253  IF (JJ)2004,2004,254
143.          254  DO 256 I=1,JJ
144.              IR=I+NDDC(NDDM)
145.              IX=IX+1
146.              NDDC(IX)=IR
147.              DO 255 J=1,2
148.                  255  DISP(IX,J)=DISP(NDDM,J)
149.          256  CONTINUE
150.          IF (IX>NNSD)2004,2002,2002
151.          2002  NLS=100
152.      C*****INITIALIZE LOAD AND STIFFNESS MATRICES TO ZERO*****
153.          KME=ANLC
154.          DO 107 I=1,NM
155.              F(I)=0.
156.          DO 107 J=1,NF
157.              107  S(I,J)=0.
158.      C*****GENERATE GLOBAL MATRICES S(I,J) AND F(I) IN BLOCKS,
159.      C          TREATING TWO BLOCKS EACH TIME *****
160.      C          SEARCH FOR ELEMENT THAT CONTRIBUTES TO UPPER BLOCK
161.      C          AND GENERATE ITS STIFFNESS AND LOAD MATRICES
162.          REWIND 10
163.          REWIND 12
164.          LYN=1
165.          NEN=0
166.          106  NEN=NEN+1
167.          NL=(NEN-1)*LLR+1
168.          NT=NEN*NL
169.          NTC=NT*NL5

```

Reproduced from
best available copy.

```

170.      GO TOE T=1,NELFM
171.      TF (NOD(I,1))105,105,105
172.      106 TN=T
173.      DO 107 J=1,4
174.      IF (NOD(I,J)*2-NT)108,108,107
175.      107 CONTINUE
176.      GO TO 105
177.      108 I1=NOD(I,1)
178.      I2=NOD(I,3)
179.      X1=.5*(RAD(I2)+RAD(I1))
180.      X2=.5*(RAD(I2)-RAD(I1))
181.      Y2=.5*(TTA(I2)-TTA(I1))
182.      TF (Y2)206,206,207
183.      206 Y2=.5*(5.28719-TTA(I1))
184.      207 Y1=TTA(I1)+Y2
185.      F=PD(I,1)
186.      PR=PD(I,2)
187.      CCR=PD(I,3)
188.      WRITE (12)IN,X1,X2,Y1,Y2,E,PR,CCR
189.      LYNC=(I-1)/NFR
190.      TF (LYNC-LYN)114,110,114
191.      114 LYN=LYNC
192.      CALL INTEG
193.      C      ADD ELEMENT STIFFNESS MATRIX INTO UPPER
194.      C      TRIANGULAR PORTION OF S(I,J)
195.      110 DO 219 K=1,4
196.      DO 219 J=1,2
197.      KN=(K-1)*2+J
198.      KM=(NOD(I,K)-1)*2+J-(NFN-1)*NLB
199.      DO 213 L=1,4
200.      IF (NOD(I,L)-NOD(I,K))213,214,214
201.      214 DO 215 MX=1,2
202.      LN=(L-1)*2+MX
203.      LM=(NOD(I,L)-NOD(I,K))*2+MX-J+1
204.      TF (LM)215,215,212
205.      212 S(KM,LM)=S(KM,LM)+SL(KN,LN)
206.      215 CONTINUE
207.      217 CONTINUE
208.      219 CONTINUE
209.      NOD(I,1)=-NOD(I,1)
210.      105 CONTINUE
211.      C*****INTRODUCE CONCENTRATED LOADS TO F(I)*****
212.      IF (NNCL)10,10,9
213.      9 DO 4 I=1,NNCL
214.      IF (NODC(I)*2-NL)4,6,5
215.      5 IF (NODC(I)*2-NT)6,6,4
216.      6 DO 7 J=1,2
217.      IF (CLOAD(I,J))8,7,8
218.      8 KM=(NODC(I)-1)*2+J-(NFN-1)*NLB
219.      F(KM)=F(KM)+CLOAD(I,J)
220.      7 CONTINUE
221.      4 CONTINUE
222.      C*****INTRODUCE BOUNDARY CONDITIONS TO S(I,J)AND F(I)*****
223.      10 DO 14 I=1,NNSD
224.      IF (NODB(I)*2-NL)14,16,15
225.      15 TF (NODB(I)*2-NT)16,16,17
226.      16 DO 15 J=1,2

```

```

227.      TF (100.-ABS(DISP(I,J)))10.10.25
228.      25 KM=(NODB(I)-1)*2+J-(NBN-1)*NLB
229.      F(KM)=DISP(I,J)
230.      S(KM,1)=1.
231.      KK=KM
232.      DO 19 K=2,NBW
233.      KK=KK+1
234.      F(KK)=F(KK)-S(KM,K)*F(KM)
235.      19 S(KM,K)=0.
236.      KK=KM
237.      DO 20 MX=2,NBW
238.      KK=KK-1
239.      TF (KK)21.21.22
240.      22 F(KK)=F(KK)-S(KK,MX)*DISP(I,J)
241.      20 S(KK,MX)=0.
242.      21 CONTINUE
243.      18 CONTINUE
244.      GO TO 14
245.      17 KRK=NODB(I)*2-NT-NBW
246.      TF (KRK)23.23.14
247.      23 DO 24 J=1,2
248.      TF (100.-ABS(DISP(I,J)))24.24.25
249.      25 KM=(NODB(I)-1)*2+J-(NBN-1)*NLB
250.      LRL=KM+1-NBW-NLB
251.      TF (LRL)28.28.24
252.      28 KK=NLB+1
253.      LIM1=KM-NLB+1
254.      DO 27 ML=LIM1,NBW
255.      KK=KK-1
256.      F(KK)=F(KK)-S(KK,ML)*DISP(I,J)
257.      S(KK,ML)=0.
258.      27 CONTINUE
259.      24 CONTINUE
260.      14 CONTINUE
261.      C.....WRITE UPPER BLOCK ON TAPE AND SHIFT UP LOWER BLOCK.....
262.      WRITE (10) (F(N),(S(N,M),M=1,NBW),N=1,NLB)
263.      IF (NTNN*2-NLE)50,50,31
264.      31 IF (NTNN*2-NT)50,50,32
265.      32 DO 33 L=1,NLB
266.      LL=L+NLB
267.      F(LL)=F(LL)
268.      F(LL)=0.
269.      DO 33 ML=1,NBW
270.      S(L,ML)=S(LL,ML)
271.      33 S(LL,ML)=0.
272.      GO TO 104
273.      C.....COMPUTE AND PRINT NODAL DISPLACEMENTS.....
274.      50 CALL DISPL
275.      IF (NLB)998,998,138
276.      138 DO 480 MJ=1,NCOU
277.      PRINT 2999,MJ
278.      2999 FORMAT (10HNO CYCLE NO.,T3)
279.      CRLF=10000000.
280.      IF (NCHO)96,95,96
281.      95 PRINT 3000
282.      3000 FORMAT (38H)      STRESS'S AT ELEMENT CENTRAL POINT)
283.      PRINT 3002

```

Reproduced from
best available copy.

```

284. 7002 FORMAT (6H ELEMENT,7H RADIAL,6X,6H CIRCUM,6X,6H SHEAR,
285. 16X,6H PRNCP1,6X,6H PRNCP2,6X,6H MAX SHR,6X,6H LO FAC)
286. 01 REXTND 12
287. 00 465 MI=1,NFLEM
288. RFAD (12) IN,X1,X2,Y1,Y2,E,PR,CCR
289. IF (NOD(IN,4)1465,52,52
290. 52 NOD(IN,1)=APS(NOD(IN,1))
291. TCR=-CCR*CTRAT
292. SCR=-CCR
293. 00 466 J=1,4
294. KP=1+(NOD(IN,J)*2-1)/NLR
295. L=(NOD(IN,J)-1)*2-NLR*(KP-2)
296. LTM2=2*J
297. LTM1=LTM2-1
298. 00 468 K=LTM1,LTM2
299. L=L+1
300. 468 F(K)=S(L,KP)
301. 466 CONTINUE
302. 00 81 I=1,4
303. 0L(I)=0.
304. 0L(I+4)=0.
305. 00 80 K=1,7,2
306. KK=K+1
307. KI=KK/2
308. 0L(I)=0L(I)+C(I,KI)*F(K)
309. 90 0L(I+4)=0L(I+4)+C(I,KI)*F(KK)
310. 81 CONTINUE
311. X(1)=GA(5)
312. Y(1)=GB(5)
313. M=1
314. N=1
315. CALL MATR
316. 00 F1 I=1,3
317. Z(I)=0.
318. 00 F0 J=1,8
319. 50 Z(I)=Z(I)+BB(I,J)*0L(J)
320. F1 CONTINUE
321. DUM1=SQRT(.25*(Z(1)-Z(2))**2+Z(3)**2)
322. DUM2=.5*(Z(1)+7*(2))
323. TS=DUM2+DUM1
324. CS=DUM2-DUM1
325. SS=DUM1
326. 7Z(IN,1)=Z(1)
327. 7Z(IN,2)=Z(2)
328. 7Z(IN,3)=Z(3)
329. 7Z(IN,4)=TS
330. 7Z(IN,5)=CS
331. 7Z(IN,6)=SS
332. 7R=1.0E-5
333. IF (TS-7R)62,62,63
334. 63 IF (CS+7R)65,67,67
335. 65 IF (CCR/CS-TCR/TS)62,67,67
336. 67 HLF=CCR/TS
337. KEF(IN)=1
338. GO TO 64
339. 52 HLF=CCR/CS
340. KEF(IN)=0

```



```

341.      64 TF (ABS(SS)-ZRIE9.F9.BF
342.      8F TF (ABS(SCR/SS)-HLF)68.E9.E3
343.      8B HLF=ABS(SCR/SS)
344.      KFF(TNI=-1
345.      69 PCR=1000.*HLF
346.      FLOF(INI)=HLF
347.      TF (NCH01 97.98.97
348.      96 PRINT 4002.IN.Z(1).Z(2).Z(3).TS.CS.SS.HLF
349.      4002 FORMAT (1E.BF12.E)
350.      37 TF (HLF-CRLF) 6E.465.465
351.      8E CRLF=HLF
352.      PCR0=PCR
353.      ND=TN
354.      46F CONTINUE
355.      TF (NCH0112E.122.12E
356.      12E PRINT 12E.PCR0
357.      12E FORMAT (17H)CRITICAL LOAD = .F12.E)
358.      122 NBK=(NWCL-1)*2/NLB+1
359.      LBK=NWCL*2-1-(NBK-1)*NLB
360.      MBK=NLB*LBK
361.      DSP=PCRG/1000.*S(MBK.NBK)
362.      PRINT 4005.DSP
363.      4005 FORMAT(12H)VERT. DTGFL. AT POINT OF LOAD =.F12.E)
364.      NBK1=(NST1-1)*2/NLB+1
365.      NBK2=(NST2-1)*2/NLB+1
366.      LBK1=NST1*2-1-(NBK1-1)*NLB
367.      LBK2=NST2*2-1-(NBK2-1)*NLB
368.      MBK1=NLB*LBK1
369.      MBK2=NLB*LBK2
370.      STR=(S(MBK2.NBK2)-S(MBK1.NBK1))/(RAD(NST2)
371.      2-RAD(NST1))*PCRG/1000.
372.      PRINT 4182.STR
373.      4182 FORMAT (20H)STRAIN AT CENTER = .F12.E)
374.      JEN=0
375.      DO 467 MK=1.NELM
376.      TF (MOD(MK,4)14E7.4E7.7E
377.      7E TRUN=(FLOF(ND)-FLOF(MK))/FLOF(ND)
378.      TF (ABS(TRUN)-TRN)77.77.467
379.      77 JFN=JFN+1
380.      NFL(JEN)=MK
381.      DO 468 MC=1.IRN
382.      TF (MK-NTK(MC)14E8.7E.468
383.      7E NAMCHA=MK
384.      GO TO 907
385.      468 CONTINUE
386.      467 CONTINUE
387.      TF (NCH0194.221).04
388.      221 PRINT 4001
389.      4001 FORMAT (75H)THE FOLLOWING ELEMENTS HAVE FAILED)
390.      GO TO 132
391.      94 PRINT 3003
392.      3003 FORMAT (34H)
393.      PRINT 3004
394.      3004 FORMAT (8H ELEMENT.7H RADIAL.6X.6H)CIRCUM.6X.6H SHEAR.
395.      10X.6H)PRNCP1.6X.6H)PRNCP2.6X.6H)MAX)SHR.6X.12H)FAILURE MODE)
396.      132 DO 469 MD=1.JFN
397.      ND=NFL(MD)

```

Reproduced from
best available copy.

```

398.
399.
400.
401.
402.
403.
404.
405.
406.
407.
408.
409.
410.
411.
412.
413.
414.
415.
416.
417.
418.
419.
420.
421.
422.
423.
424.
425.
426.
427.
428.
429.
430.
431.
432.
433.
434.
435.
436.
437.
438.
439.
440.
441.
442.
443.
444.
445.
446.
447.
448.
449.
450.
451.
452.
453.
454.
455.
456.
457.
458.
459.
460.
461.
462.
463.
464.
465.
466.
467.
468.
469.
470.
471.
472.
473.
474.
475.
476.
477.
478.
479.
480.
481.
482.
483.
484.
485.
486.
487.
488.
489.
490.
491.
492.
493.
494.
495.
496.
497.
498.
499.
500.
501.
502.
503.
504.
505.
506.
507.
508.
509.
510.
511.
512.
513.
514.
515.
516.
517.
518.
519.
520.
521.
522.
523.
524.
525.
526.
527.
528.
529.
530.
531.
532.
533.
534.
535.
536.
537.
538.
539.
540.
541.
542.
543.
544.
545.
546.
547.
548.
549.
550.
551.
552.
553.
554.
555.
556.
557.
558.
559.
560.
561.
562.
563.
564.
565.
566.
567.
568.
569.
570.
571.
572.
573.
574.
575.
576.
577.
578.
579.
580.
581.
582.
583.
584.
585.
586.
587.
588.
589.
590.
591.
592.
593.
594.
595.
596.
597.
598.
599.
600.
601.
602.
603.
604.
605.
606.
607.
608.
609.
610.
611.
612.
613.
614.
615.
616.
617.
618.
619.
620.
621.
622.
623.
624.
625.
626.
627.
628.
629.
630.
631.
632.
633.
634.
635.
636.
637.
638.
639.
640.
641.
642.
643.
644.
645.
646.
647.
648.
649.
650.
651.
652.
653.
654.
655.
656.
657.
658.
659.
660.
661.
662.
663.
664.
665.
666.
667.
668.
669.
670.
671.
672.
673.
674.
675.
676.
677.
678.
679.
680.
681.
682.
683.
684.
685.
686.
687.
688.
689.
690.
691.
692.
693.
694.
695.
696.
697.
698.
699.
700.
701.
702.
703.
704.
705.
706.
707.
708.
709.
710.
711.
712.
713.
714.
715.
716.
717.
718.
719.
720.
721.
722.
723.
724.
725.
726.
727.
728.
729.
730.
731.
732.
733.
734.
735.
736.
737.
738.
739.
740.
741.
742.
743.
744.
745.
746.
747.
748.
749.
750.
751.
752.
753.
754.
755.
756.
757.
758.
759.
760.
761.
762.
763.
764.
765.
766.
767.
768.
769.
770.
771.
772.
773.
774.
775.
776.
777.
778.
779.
780.
781.
782.
783.
784.
785.
786.
787.
788.
789.
790.
791.
792.
793.
794.
795.
796.
797.
798.
799.
800.
801.
802.
803.
804.
805.
806.
807.
808.
809.
810.
811.
812.
813.
814.
815.
816.
817.
818.
819.
820.
821.
822.
823.
824.
825.
826.
827.
828.
829.
830.
831.
832.
833.
834.
835.
836.
837.
838.
839.
840.
841.
842.
843.
844.
845.
846.
847.
848.
849.
850.
851.
852.
853.
854.
855.
856.
857.
858.
859.
860.
861.
862.
863.
864.
865.
866.
867.
868.
869.
870.
871.
872.
873.
874.
875.
876.
877.
878.
879.
880.
881.
882.
883.
884.
885.
886.
887.
888.
889.
890.
891.
892.
893.
894.
895.
896.
897.
898.
899.
900.
901.
902.
903.
904.
905.
906.
907.
908.
909.
910.
911.
912.
913.
914.
915.
916.
917.
918.
919.
920.
921.
922.
923.
924.
925.
926.
927.
928.
929.
930.
931.
932.
933.
934.
935.
936.
937.
938.
939.
940.
941.
942.
943.
944.
945.
946.
947.
948.
949.
950.
951.
952.
953.
954.
955.
956.
957.
958.
959.
960.
961.
962.
963.
964.
965.
966.
967.
968.
969.
970.
971.
972.
973.
974.
975.
976.
977.
978.
979.
980.
981.
982.
983.
984.
985.
986.
987.
988.
989.
990.
991.
992.
993.
994.
995.
996.
997.
998.
999.
1000.

```

Reproduced from
best available copy.

```

451.      SL(KP,L)=0.
452.      SL(L,KP)=0.
453.      71 CONTINUE
454.      45 CONTINUE
455.      47 CONTINUE
456.      48 CONTINUE
457.      DO 75 K=1,4
458.      DO 72 J=1,2
459.      KN=(K-1)*2+J
460.      KM=(NOD(ND,K)-1)*2+J-(NNB-1)*NLB
461.      DO 73 L=1,4
462.      IF (NOD(ND,L)-NOD(ND,K))173,74,74
463.      74 DO 75 MX=1,2
464.      LN=(L-1)*2+MX
465.      LM=(NOD(ND,L)-NOD(ND,K))*2+MX-J+1
466.      IF (LM)75,75,72
467.      72 S(KP,LM)=S(KM,LM)-.9*SL(KN,LN)
468.      75 CONTINUE
469.      73 CONTINUE
470.      74 CONTINUE
471.      BACKSPACE 20
472.      WRITE (10) (F(N),(S(N,M),M=1,NBW),N=1,NLB)
473.      IF (NNB-NBN)82,82,82
474.      82 WRITE (10) (F(N),(S(N,M),M=1,NBW),N=N1,N2)
475.      BACKSPACE 10
476.      DO 175 K=1,MILA
477.      READ (10) (F(N),(S(N,M),M=1,NBW),N=1,NLB)
478.      175 CONTINUE
479.      82 NOD(ND,4)=-NOD(ND,4)
480.      469 CONTINUE
481.      CALL DISPL
482.      IF (NLB)998,998,430
483.      460 CONTINUE
484.      GO TO 998
485.      997 PRINT 25E,NAMCHA
486.      290 FORMAT (8H ELEMENT,T4,
487.      14H WHICH IS IN VICINITY OF LOAD HAS FAILED/
488.      118H RUN IS TERMINATED)
489.      998 STOP
490.      FND
491.
492.
493.
494.
495.
.....

```

END OF COMPILATION:

NO DIAGNOSTICS.

```

1.      SUBROUTINE DTSP
2.      COMMON/COLOC/NROW,MM,NUMBLK,NFG,B(200),A(200,100)
3.      ZR=1.0E-6
4.      NN=NFG
5.      NF=1
6.      NH=NN+NN
7.      MT=NFG
8.      ML=NN+1
9.      NU=1
10.     IF (NUMBLK-1)G1,155,G1
11.     G1 REWIND 11
12.     REWIND 10
13.     NS=0
14.     GO TO 1FD
15.     C REDUCE EQUATIONS BY BLOCKS
16.     C 1. SHIFT BLOCK OF EQUATIONS
17.     100 NS=NS+1
18.     DO 125 N=1,NN
19.     NM=NN*N
20.     B(N)=R(NM)
21.     R(NM)=0.
22.     DO 125 M=1,MM
23.     A(N,M)=A(NM,M)
24.     125 A(NM,M)=0.
25.     C 2. READ NEXT BLOCK INTO CORE
26.     IF (NUMBLK-NS)150,155,150
27.     150 READ (10) (B(N),(A(N,M),M=1,MM),N=ML,NH)
28.     IF (NB)154,100,154
29.     C 3. REDUCE BLOCK OF EQUATIONS
30.     155 MT=NROW*2-(NUMBLK-1)*NFG
31.     NF=0
32.     154 DO 380 N=1,MT
33.     C CHECK FOR VERY SMALL OR ZERO ELEMENT ON DIAGONAL
34.     CH=0.
35.     DO 165 M=1,MM
36.     IF (CH-ABS(A(N,M)))194,165,165
37.     94 CH=ABS(A(N,M))
38.     165 CONTINUE
39.     XXX=ABS(A(N,1))/CH
40.     IF (XXX-ZR)95,95,299
41.     C IF ZERO OR SMALL ON DIAGONAL TERMINATE RUN
42.     95 PRINT 2300,XXX,N,NS
43.     2300 FORMAT (79H SMALL DIAGONAL - A(N,1)/MAX A(N,M) IS
44.     1F14.4,12H IN EQUATION,14,9H OF BLOCK,14)
45.     NF=0
46.     GO TO 90
47.     C NORMAL ELIMINATION PROCEDURE
48.     200 R(N)=R(N)/A(N,1)
49.     DO 375 L=2,MM
50.     IF (ABS(A(N,L))-ZR)375,375,376
51.     376 C=A(N,L)/A(N,1)
52.     TEN=L-1
53.     J=0
54.     DO 370 K=L,MM
55.     J=J+1

```

Reproduced from
best available copy.

```

56.      350 A(I,J)=A(I,J)-C*A(N,K)
57.      B(I)=B(I)-A(N,L)*B(I)
58.      A(N,L)=C
59.      375 CONTINUE
60.      780 CONTINUE
61.      C      WRITE BLOCK OF EQUATIONS ON TAPE 11
62.      IF (NUMBLK-NB) 84, 400, 84
63.      84 WRITE (11) (B(N), (A(N,M), M=1, MM), N=1, NN)
64.      GO TO 100
65.      C      BACK-SUBSTITUTION
66.      400 DO 450 M=1, MT
67.      N=MT+1-M
68.      L1=2
69.      87 DO 435 K=L1, MM
70.      L=N+K-1
71.      425 B(N)=B(N)-A(N,K)*B(L)
72.      450 CONTINUE
73.      ME=NR+1
74.      DO 460 N=1, MT
75.      NM=N+NN
76.      A(NM, NR)=B(N)
77.      IF (NB-NUMBLK) 70, 460, 460
78.      70 A(NM, ME)=B(NM)
79.      460 B(NM)=B(N)
80.      NB=NR-1
81.      IF (NB) 500, 500, 71
82.      71 BACKSPACE 11
83.      MT=NN
84.      READ (11) (P(N), (A(N,M), M=1, MM), N=1, NN)
85.      BACKSPACE 11
86.      GO TO 400
87.      500 K=1
88.      NMI=NEU-1
89.      DO 600 I=1, NROW
90.      NMI=NMI+2
91.      NMF=NMI+1
92.      IF (NMF-2.*NFW) E(2, EU2, F(1)
93.      600 K=K+1
94.      NMI=NEU+1
95.      NMF=NMI+1
96.      602 CONTINUE
97.      600 CONTINUE
98.      90 RETURN
99.      END
100.      C*****
101.      C*****

```

Reproduced from
best available copy.

END OF COMPILATION:

NO DIAGNOSTICS.

```

1.      SUBROUTINE MATE
2.      COMMON/JACKP/C(4,4),R(3,8),FL(8),SL(2,8),RR(3,8)
3.      COMMON/BCFAP/PR,E,T,TCR,CCR
4.      COMMON/KRING/X1,X2,Y1,Y2,X(3),Y(3),Z(3),M,N
5.      RR=X1+X2*X(M)
6.      DUM=E*T/(1.-PR*PR)
7.      XX=X(M)
8.      YY=Y(N)
9.      R(1,2)=1./X2
10.     R(1,4)=YY/X2
11.     R(2,1)=1./RR
12.     R(2,2)=XX/RR
13.     R(2,3)=YY/RR
14.     R(2,4)=XX*YY/RR
15.     R(2,7)=1./RR/Y2
16.     R(2,8)=XX/RR/Y2
17.     R(3,7)=R(2,7)
18.     R(3,4)=R(2,8)
19.     R(3,5)=-R(2,1)
20.     R(3,6)=1./X2-XX/RR
21.     R(3,7)=-R(2,7)
22.     R(3,8)=YY*R(3,6)
23.     DO 25 I=1,8
24.     RB(1,I)=DUM*(R(1,I)+PR+R(2,I))
25.     RR(2,I)=DUM*(R(2,I)+PR+R(1,I))
26.     RB(3,I)=DUM*.5*(1.-PR)*R(3,I)
27.     25 CONTINUE
28.     RETURN
29.     END

```

Reproduced from
best available copy.

END OF COMPILATION:

NO DIAGNOSTICS.

```

1.      SUBROUTINE INTFG
2.      COMMON/JAKF/C(4,4),R(7,8),FL(8),SL(8,8),BR(3,8)
3.      COMMON/KRING/X1,X2,Y1,Y2,X(T),Y(3),Z(3),M,N
4.      DIMENSION H(3),AA(3),DL(8),D(3,8),DX(3,8)
5.      DATA (H(I),I=1,3)/.55555555,.88888888,.55555555/
6.      DATA (AA(I),I=1,3)/-.775,0.,.775/
7.      DO 3 T=1,8
8.      DL(I)=0.
9.      FL(T)=0.
10.     DO 4 K=1,8
11.     4 DX(T,K)=0.
12.     DO 5 J=1,8
13.     C(I,J)=0.
14.     5 SL(J,I)=0.
15.     3 CONTINUE
16.     DO 31 L=1,3
17.     M=L
18.     X(M)=AA(M)
19.     RR=X1+X2*X(M)
20.     DO 30 J=1,3
21.     N=J
22.     Y(N)=AA(N)
23.     CALL MATP
24.     DUM1=H(L)*H(J)*RR*X2*Y2
25.     DO 20 NROW=1,8
26.     DO 20 NCOL=NRWX,8
27.     DUM2=0.
28.     DO 10 KK=1,3
29.     10 DUM2=DUM2+R(KK,NROW)*BR(KK,NCOL)
30.     20 D(NROW,NCOL)=D(NROW,NCOL)+DUM2*DUM1
31.     30 CONTINUE
32.     31 CONTINUE
33.     DO 6 I=1,7
34.     J=I+1
35.     DO 6 K=0,8
36.     6 D(K,I)=D(I,K)
37.     I1=-1
38.     DO 25 I=1,8
39.     T1=I+1
40.     T2=(T-1)/2+1
41.     DO 24 J=1,3
42.     DO 23 K=1,4
43.     K1=K+I1+4
44.     23 DX(I,J)=DX(T,J)+C(K,T2)*D(K1,J)
45.     24 CONTINUE
46.     TF=(I1-1)*25,21,21
47.     21 I1=-1
48.     25 CONTINUE
49.     I1=-1
50.     DO 28 I=1,8
51.     I1=I+1
52.     T2=(T-1)/2+1
53.     DO 27 J=1,8
54.     DO 26 K=1,4
55.     K1=K+I1+4

```

```
FC.      2E SL(J,I)=SL(J,I)+DX(J,K)*C(K,I2)  
FD.      27 CONTINUE  
FE.      2F (T1-I)20,27,22  
FF.      22 T1=-1  
GD.      2B CONTINUE  
HD.      2D 7 I=1,7  
ID.      J=I+1  
JD.      2D 7 K=J,6  
LD.      7 SL(I,K)=SL(K,I)  
MD.      RETURN  
ND.      END
```

END OF COMPILATION: NO DIAGNOSTICS.

Reproduced from
best available copy.


```
1.      SUBROUTINE UNIFORM(A,B,C)
2.      D=PI*UNIF(R)
3.      C=A+(B-A)*D
4.      RETURN
5.      END
```

END OF COMPILATION: NO OPTIMISTICS.

Reproduced from
best available copy.